UNIVERSITY OF OKLAHOMA

GRADUATE COLLEGE

HYBRID ACTIVE-PASSIVE RFID TAG FOR TRACKING BIRDS USING EXISTING RADAR SYSTEMS

A THESIS

SUBMITTED TO THE GRADUATE FACULTY

in partial fulfillment of the requirements for the

Degree of

MASTER OF SCIENCE

By

ZACHARY POTTS

Norman, Oklahoma

2019

HYBRID ACTIVE-PASSIVE RFID TAG FOR TRACKING BIRDS USING EXISTING RADAR SYSTEMS

A THESIS APPROVED FOR THE
SCHOOL OF ELECTRICAL AND COMPUTER ENGINEERING

BY

Dr. Caleb J. Fulton, Chair

Dr. Jessica Ruyle

Dr. Hjalti Sigmarsson

© Copyright by Zachary Potts 2019
All Rights Reserved.

Table of Contents

List of Tables

List of Figures

Abstract

RFID "radio-frequency identification" tags are a powerful tool for the identification and tracking of objects across a variety of media. RFID tags have applications in security badges, individual identification tags, short range tracking systems, and other similar devices. These applications are all relatively short range, r, ($r < 100$) m and thus require low power. Through the use of the WSR-88d (NEXRAD) weather radar system this technology can potentially be extended to long range ($r > 100$) km applications. With the WSR-88d's large realized gain of 45.5 dB and high transmitted power 700 kw it is possible to achieve a bird tracking device that can be passively used with the already developed weather infrastructure. The solution is realized as a small form factor enclosure that is attached to the animal being observed. Each individual tag represents an unique identifier that can distinguish it from the other versions of the tag. The transmitter's portion of the tracking procedure is done by observing the unique coded back scatter of each individual tag via the WSR-88d's pulses to check the location and path of the animal as it travels across the United States. In this study, an RFID tag compatible with the NEXRAD weather radar network is produced. This tag demonstrates the ability to backscatter pulse-to-pulse across the entire pulse repetition frequency range of the NEXRAD network. Multiple modulation schemes are presented and detailed in the results chapter. These modulation schemes are demonstrated across a variety of power

ranges as well to insure functionality as the bird changes distance from the radar.

Chapter 1

Introduction

Throughout history there has been a desire to study the migratory patterns of animals. Typically this has been done using GPS trackers, short range radio transmitters, and metal identification bands that must be manually recorded at the origin and final location.[1] With the advancement of radar technology there is a new possibility in using long ranged (100+ km) Radio-Frequency Identification Tags (RFID) in unison with high power established weather radar infrastructure. This infrastructure is the Next-Generation Radar (NEXRAD) network operated and maintained by the National Weather Service (NWS), which is part of the National Oceanic and Atmospheric Administration (NOAA), as well as the Federal Aviation Administration (FAA), the Department of Transportation, and the U.S. Air Force. In particular, the NEXRAD system is a network of 160 S-band Doppler radars scattered throughout the United States as seen in Figure 1.1-[2]. Currently, there are many deficiencies within the standard methods of tracking birds. Light sensing geolocators are one of the current popular solutions[1]. These geolocators require specific conditions to work due to their reliance on determining the path of the animal by the direction of the sunlight and the sunlight's intensity. Some of the complications presented by

this solution are that birds that migrate during equinoxes or other periods of poor lighting, which creates poor data quality. Tags must also be retrieved at the end of the migration periods since there is no transmitter. Another potential source of error is that longitudinal pathways present issues as it is hard to determine light differences and changes in flight location when the bird follows these lines. Finally, the overall flight path is considered just an estimation since exact range, distance, and location can only be estimated by these tags. Another popular option is Global Positioning System (GPS) tracking. GPS based tags offer great quality in the positional, directional, and speed tracking categories. Currently, these GPS tags have a much higher cost when compared to metal bands and geolocators[1]. Where these tags struggle, is that they don't provide continual streamed information. The tags can provide a well defined and detailed flight pattern, but not real time updates and the tags have had issues with a higher fail rate than other mediums in the past. The third popular option is short range radio tags. Improving these tags and their associated range is the focus of this study. In their current form, these tags suffer from a lack of transmission towers, relatively high cost per unit, and a short battery life. However, A large benefit of these radio tags is that past studies have shown a much higher recovery rate of the tags compared to other methods, making them a cheaper solution if they can be recovered. The proposed tag made of components off-the-shelf (COTS) and an established transmission system provides answers to two of the tags problems. Future work involves the possibility of RF energy harvesting to charge the tag's batteries to solve the third issue. Overall, these radio tags have shown to be a good compromise between quality of data, price, and longevity[1].

The motivation for a combination of a cheap and reliable tracking option with

minimal downtime and maximum range is the driving force behind this study. The proper combination of these requirements could allow for continuous migratory tracking from any location. With the online free NOAA website, data is easily accessible for any WSR-88d location at a variety of time periods[3]. The proposed radar based tracking system provides a simple solution by pairing cheap and reliable RFID tags with an established and maintained weather radar system. This solution would uniquely benefit from the extremely high power by the NEXRAD network's radars in comparison to typical UHF RFID transmitters that are capped by a 4 Watt maximum in the United States of America[4]. The demand of a virtually permanent up time and minimal blind spot system at a low price point has lead to an increased interest in funding a proper solution. In comparison to current technology, this study's proposed tag can potentially meet these demands for tracking North America migration patterns reliably and cheaply. The other distinct advantage to using the WSR88-D radars from NOAA's NEXRAD weather radar system is the large quantity of radars strategically spread across the 48 contiguous United States as seen in Fig 1.1. There is a consistent blanket of coverage for tracking animals within the United States with minimal blind spots located mostly around the Rocky Mountains. While the functionality of these tags decreases exponentially with range, the sheer amount of power transmitted allows for these new "long range RFID tags"[5].

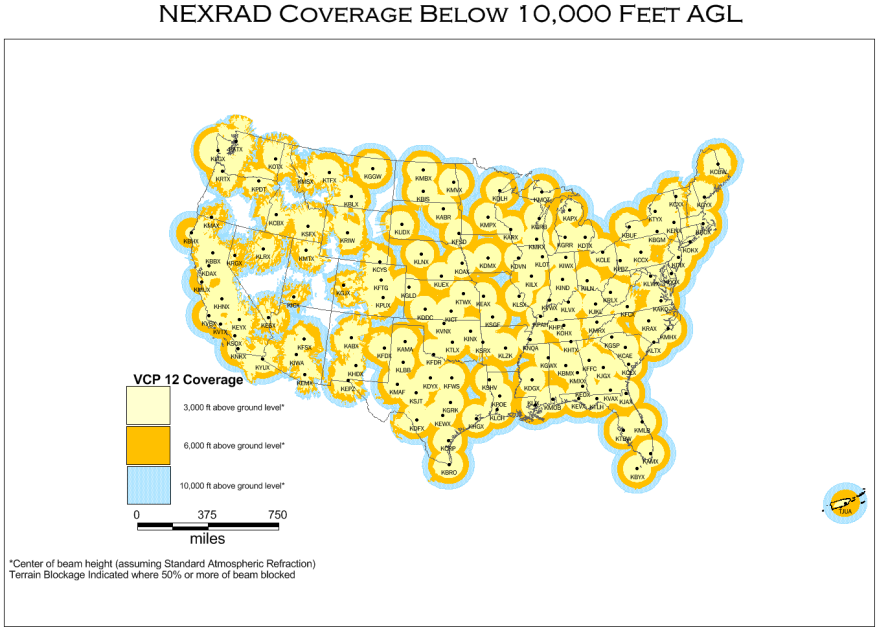

Figure 1.1: A coverage map of the NEXRAD radar system across the contiguous United States created by NOAA [6].

1.1 A brief history of RFID

The theory that RFID communication was designed on was first submitted by Harry Stockman in 1948[7]. The theory presented was unable to be realized in practice at that point in history and it was noted that a considerable amount of work must be done on developing the technology. In 1964, R.F. Harrington studied and produced a paper on the theory of loaded scatterers[8]. In the late 1960's several of the first large RFID producing companies were founded. The largest initial use of RFID tags was as anti theft clothing tags. Knogo created electronic article surveillance (EAS) tags for this purpose. In 1970, RFID were becoming more popular and the technology was even being developed at the Los Alamos Scientific Laboratory[9]. From their research at Los Alamos, Alfred Koelle, Steven Depp, and Robery Freyman published in 1975 their paper on the short range identification of devices using modulated backscatter[10]. Raytheon released their Raytag in 1973 while RCA began developing an electronic identification system in 1975[9]. In the 1980's RFID technology became implemented in a much larger scale across the world. In 1987, the first commercial application of RFID for collecting tolls to use public transportation began in Norway. A few years later in 1989 the Dallas North Turnpike began using RFID tags as well[9]. In 1991, Oklahoma opened the first ever open highway electronic tolling system, Pikepass. In 1992, Houston created the first toll collection and traffic management system[9]. Later both Kansas and Georgia would create electronic highway toll sytems that were compatible with Oklahoma through the Title 21 standard[9]. Also in the 1990's, Texas Instruments began development on a system used to start motor vehicles through the detection of a nearby RFID identifier[9]. Throughout the 2000's, RFID technology has been expanded greatly

in the fields previously mentioned, as well as the standards associated with their use. The goal of this study is to continue with the development of RFID tags and introduce Stockman's original theory to a long range application.

1.2 RFID Systems

Similar to typical radar applications, RFID systems consist of an object of interest, a transmitter, and a receiver. The transmitter and receiver can be the same device, or their can be a separate device for each function. When RFID systems are designed, the power calculations are based on one of these two transmitter and receiver location setups[11]. In this study, the system is specified to operate with the all-in-one transceiver setup using the WSR-88d. The system operates by the transmitter sending out pulses and either receiving the pulses back or receiving a specified response pulse generated by the RFID tag. Depending on the type of RFID tag that are discussed in the next section, the transmitter either receives a backscattered version of its pulse or a new pulse generated by the tag itself. Due to the generic requirements to be considered an RFID system, there are very many different configurations that qualify. This study focuses on a hybrid system that is activated pulse-to-pulse by the WSR-88D acting as the transceiver and backscatters onto the pulses instead of creating its own pulse. Currently, the system is programmed in a 1-bit configuration, but examples are shown to demonstrate that N-bit configurations are possible. Every other pulse is modulated to demonstrate the ability to backscatter at 2.85 GHz, as well as, other unique patterns are also demonstrated to present flexibility in design choices. Similarly, the pulses being scattered range from 300 Hz to 1.3 kHz apart to fully show the capabilities of one device being able to operate across

the WSR-88D's entire pulse repetition frequency (PRF) range[12].

RFID technology has a variety of fundamental challenges and complications associated with creating a reliable network. Since many applications of RFID involve security procedures with the RFID card being a unique identifier for some purpose, it is imperative to keep the transmission confidential or encrypted. Violating the RFID network can be done several ways, through intercepting the communication either direction, or through a different transmitter copying the desired pulse frequency and pattern and interrogating the RFID tag itself[13]. For the purpose of RFID tracking with the current aperture this is not a problem. Total privacy is not needed and the nature of the birds being airborne a majority of the time mitigates the necessity of a confidential system. Another challenge associated with RFID is interference from a variety of sources. Some of these situations are unavoidable, in a scenario where a large majority of tags are clustered in a singular area there will be an overlap in backscatter generated by each tag and they will interfere with each other inside the resolution range of the WSR-88d. Again, due to the nature of birds being continually airborne, ground clutter will be mostly irrelevant as a source of interference with tracking the proposed tag. Almost all of the interference seen should be common enough that it has already been mitigated by the WSR-88d's system while tracking weather.

1.3 Types of RFID tags

RFID tags are classified as either active, passive, or hybrid tags. Passive tags do not have an internal power source and rely on their associated transmitter for all of their power. Passive tags operate by modulating the pulse produced by the trans-

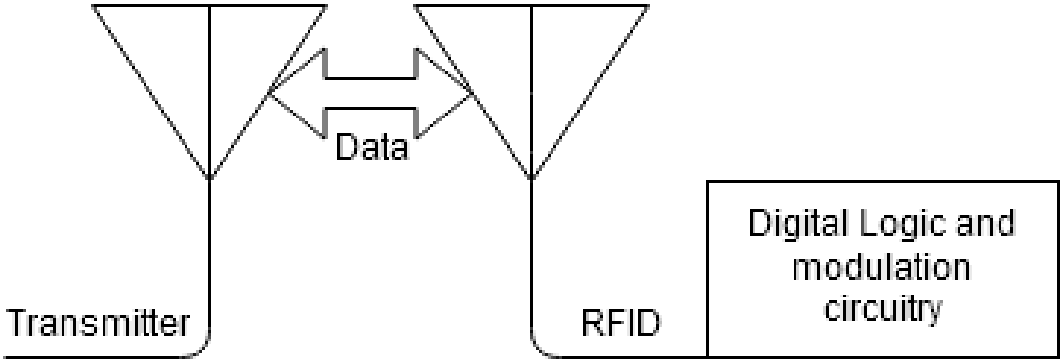

Figure 1.2: An example of a generic RFID system.

mitter and storing the energy into a temporary battery via an RF harvesting circuit to ensure the backscatter and interrogation systems work correctly and the right modulation is done on the incoming pulse. Passive tags have the advantage over other types of RFID tags of only needing the transmitter in range to fully function. By having the transmitter send and receive data through its pulses and the tag not requiring a battery, passive tags always work while within the transmitter's range. Once the passive tag leaves the ideal range for power harvesting, it becomes inert until it reenters the transmitter's range. These tags are the most commonly used form of RFID.[12]

Active RFID tags differ by having an on-board power source. This source can have a variety of potential uses for the system. Common uses are powering the logic that stores the backscatter pattern and sequence, powering low noise amplifiers, or manually toggling switches for backscatter. The biggest advantage of having an on-board power source is the ability to amplify the transmitter's signal. This allows the RFID tag to be located much farther from the transmitter giving the system more total range. Additionally, the system can also function without the transmitter's pulse activating the tag. If the system uses a timer, the pulse is only needed to

observe the backscatter of the tag, but not activate it. Another form of active RFID tags involves the RFID having its own transmission chain. It utilizes the on-board power source to power the tag's amplifier, signal generator, and digital logic instead of modulating the signal it receives. As noted in the RFID handbook, these devices are better named short-range radio devices instead of RFID tags as they operate on their own and are just observed by the transmitter[12], [14].

Hybrid RFID tags operate by utilizing backscatter modulation, but also have a power source for other features. Hybrid tags still remain true RFID devices by not generating their own pulse. This study involves the creation and testing of a hybrid style tag that uses the power supply to amplify the incoming signal, operate the digital logic, and toggle the switches used for modulation. By using lower power requirement parts, batteries can last for a relatively long time of a few months with no charging, while allowing the tag to have a high level of functionality and extending the total range of the device. For the design of this study, a hybrid style RFID was chosen specifically to extend the potential range of the design and to allow a more complex backscatter program by modulating multiple switches that have their own unique impedance. The ability to encode more unique patterns allows for easier determination of where each unique bird is actively located, especially when they are grouped in close proximity. Additionally, the unique codes allow for easier detection as these long code sequences are distinguished from regular radar traffic and noise[15], [16].

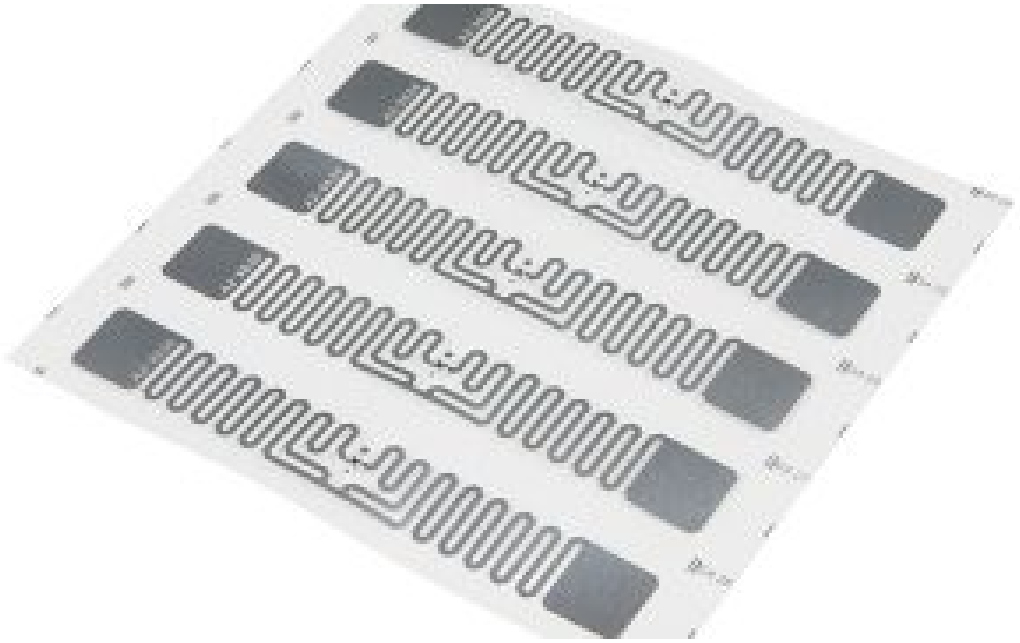

Figure 1.3: A commercially available passive RFID tag [17].

1.4 Backscatter Modulation

Backscatter is defined as when an incident wave impinges upon a passive object where the purpose is not to extract energy from the incident waves, but to detect the scattered field[18]. This backscatter cross section is used to measure how detectable a target object will be by a radar. By observing the backscatter cross section of our target RFID tag, we can determine the location, speed, direction, and identification of the animal being tracked after a few pulse strings have been modulated. Through the use of selected backscatter patterns by choosing a particular sequence of bits, information can be encoded that is seen by the radar through a series of pulses.

Backscatter modulation was originally described as point-to-point communication where the carrier power was generated by the transmitter and the receiving end has a modulating reflector instead of another transmitter[7]. The theory was that

radio, light, or sound waves could be used as the transmission wave under conditions of specular reflection. By observing the reflection coefficient between the transmitter's antenna and the receiver's load, it is possible to see different modulation patterns by actively changing the receiver's load. When the load changes the reflection coefficient of the system will also change. Through these changes we can observe the predetermined modulation schemes[7]. It is possible to change the amplitude, phase, or frequency of the transmitted signal. This study focuses on the simplest form of backscatter modulation, amplitude shift keying (ASK), but also provides proof of concept for other forms of modulation.

Amplitude Shift Keying is a modulation scheme based on the carrier signal oscillating between two states at a predetermined duty factor. The simplest form of this is to have half of the duty cycle be full amplitude (logical 1) and have the other half be at zero amplitude (logical 0). This allows the sender to create a binary code pulse to pulse between a starting and stopping predetermined padding to indicate a unique code is about to be sent[12]. Other forms of modulation include Phase Shift Keying (PSK) and Frequency Shift Keying (FSK). PSK involves modulation via changing the phase of the backscattered wave, and FSK involves changing the frequency of the backscattered wave. PSK is later briefly mentioned and an example solution is given, FSK is not discussed further in this study.

1.5 Proposed RFID Tag

This study showcases a fully integrated 2.85 GHz hybrid RFID tag that demonstrates pulse-to-pulse modulation capabilities via backscatter for use on the NEXRAD weather radar network. The study also includes examples of other modulation

schemes to demonstrate flexibility in modulation scheme design. Specifically, the demonstrated tag is capable of working across the entire NEXRAD frequency range of 2.8 GHz to 2.9 GHz range as well as being capable of handling the entire pulse repetition frequency range that the network covers. Additionally, examples are show that the proposed tag is capable of operating across the entire PRF band used by the NEXRAD system as well. By supporting pulse-to-pulse handling, the tag is capable of handling consecutive pings by different radars in the network. Chapter 2 details the tag's backscatter functionality, how it is achieved, and specifies in detail with system diagrams, the power consumption, s-parameters, and additional technical details. Chapter 3 encompasses backscatter, the antenna matching, and the band pass filter used. Chapter 3 also describes how the whole system affects the outputted pulses that create the backscatter modulation schemes. Chapter 4 covers the digital logic and envelope detection used for rectifying the WSR-88d's pulse and using it as the trigger for the RFID tag. Finally, Chapter 5 discusses the final product, a system demonstration, and entails potential future work and considerations.

Perhaps most importantly, the proposed tag would not interfere with typical WSR-88d daily use and weather tracking capabilities. Through the use of modulation schemes, the Doppler spectrum return from the RFID tag is directly affected. For example, applying a modulation scheme an encoding "1's and -1's" alternating every other pulse creates a frequency shift on the returning pulse train of half the Nyquist rate of the interrogating pulse. When observing the RFID tag over a pulse train, the backscattered return pulse will not overlap with the weather in the immediate area. There is a potential for the backscattered return pulse to overlap with weather that is half the Nyquist rate away on the Doppler spectrum, but over a series

of pulse trains the RFID tag's behaviour will be inconsistent with the surrounding weather and can then be subtracted from the data so that the weather can be clearly seen. When observing a moving target, the corresponding Doppler spectrum of that target will show the same half Nyquist rate shift plus or minus some velocity shift.

The previously mentioned frequency shift can be seen in figure 1.4 which is the Fast Fourier transform (FFT) of the square wave in figure 1.5. The center pulse can clearly be seen at the center of the sampling frequency instead of positioned at 0.

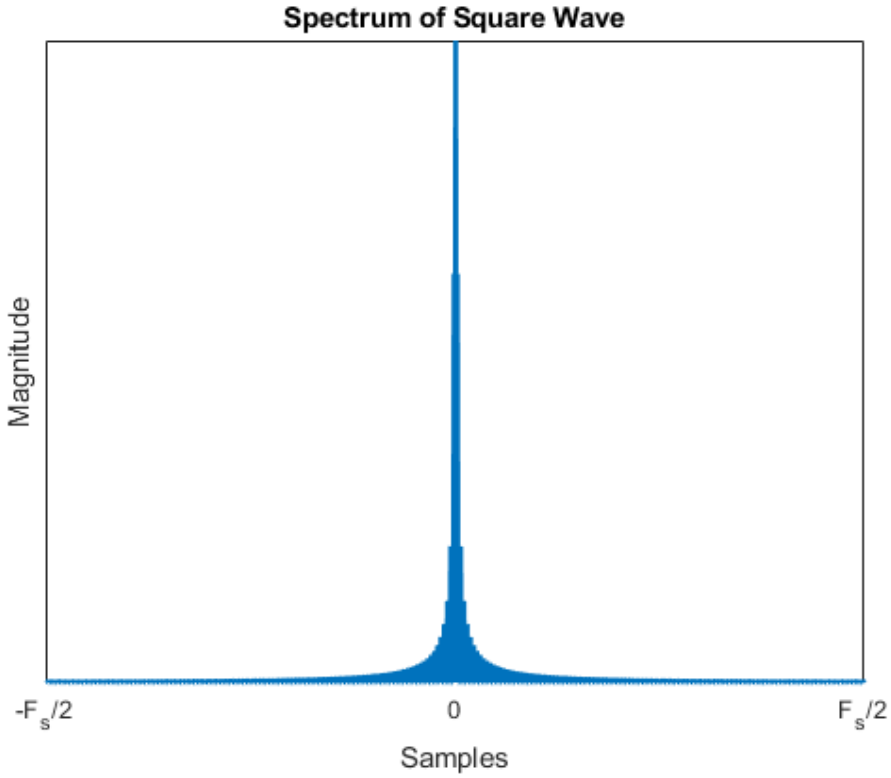

Figure 1.4: The FFT of the basic square wave example

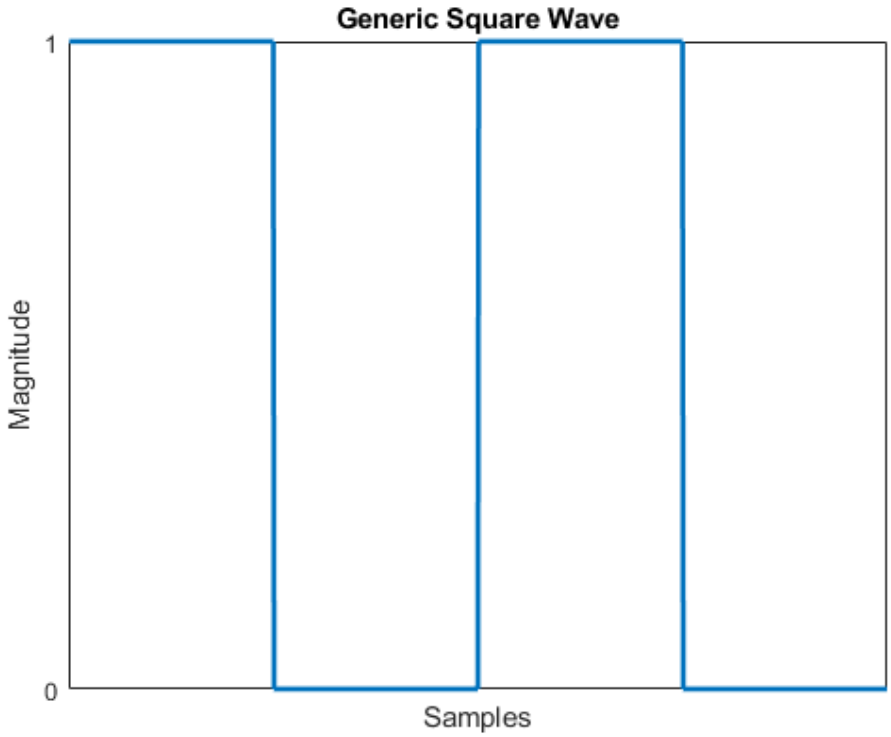

Figure 1.5: A basic square wave example.

1.6 FCC Regulations and License

In the FCC's Manual of Regulations and Procedures for Federal Radio Frequency Management there are three footnotes related to the implementation of devices like RFID tags in the frequency range of 2700-2900 MHz[19]. Footnotes 5.337 and 5.377a state:

> 5.337: The use of the bands 1300-1350 MHz, 2700-2900 MHz and 9000-9200 MHz by the aeronautical radionavigation service is restricted to ground-based radars and to associated airborne transponders which transmit only on frequencies in these bands and only when actuated by radars operating in the same band.
>
> 5.337A: The use of the band 1300-1350 MHz by earth stations in the radionavigation-satellite service and by stations in the radiolocation service shall not cause harmful interference to, nor constrain the operation and development of, the aeronautical-radionavigation service.

The additional footnote in the Manual of Regulations and Procedures for Federal Radio Frequency Management states:

> US18: In the bands 9-14 kHz, 90-110 kHz, 190-415 kHz, 510-535 kHz, and 2700-2900 MHz, navigation aids in the U.S. and its insular areas are normally operated by the Federal Government. However, authorizations may be made by the FCC for non-Federal operations in these bands subject to the conclusion of appropriate arrangements between the FCC and the Federal agencies concerned and upon special showing

> of need for service which the Federal Government is not yet prepared to render.

It follows, that for implementation of the proposed RFID system and deployment of the developed tag, that Federal operations are allowed to operate in the bands with permission and no special license are required. Coordination with the other complying departments of the government would be required by the United States Geographical Service.

Chapter 2

Typical RFID functions and considerations

2.1 Introduction

The use of RFID tags has been rapidly expanding in recent years, due to their cheap cost and small form factor the tags can easily be used for a variety of services. The ability to create a unique identification code and imprint it into a small physical device allows for these tags to have a large market in the security field. Personal identification badges for personnel, storage container labeling, and tracking tags are just a few examples of these uses. The ability to create security systems that rely specifically on exact identification codes being received allows for RFID tags to be used with strict security protocols if desired. This premise can be expanded upon to provide a unique identification code to each RFID tag for this study's goal of tracking individual birds. Overall, the desire of a cheap, long range tracking solution for researching migratory patterns of large birds has lead to the development of this study's solution. The creation of a real time system that can actively track second by second flight patterns can provide a new quality of information to researchers they have not had before and allow for new discoveries.

2.2 Function of the RFID Tag

The proposed tag operates by receiving a pulse from the WSR-88d and processing the received RF pulse through an RF to DC envelope detector. In chapter 4, calculations are done to show that the minimal detectable signal for the system is -20 dBm. After being enveloped detected, the new square wave is used as a trigger for the digital logic. Finally, the square wave's logical 1's and 0's causes the counter integrated chip (IC) to modulate the switch in a pre-desired pattern. The design of the switch section follows the classic RFID technique of modulating the tag's impedance so that a specific amount of power is reflected due to unmatched loads. This reflected power is then re-radiated by the antenna and picked up by the radar as backscatter. In the proposed configuration there are examples to show the difference from when the tag is modulated between reflecting and absorbing mode. Additionally, there are multiple examples to illustrate how changing the terminated load's impedance also greatly affects the amount of backscattered energy. On the radar's end, the reflected power will appear as an object with a high radar cross section, but will disappear every other pulse due to the modulation scheme. With the chosen modulation scheme for the tag operating on an every other pulse modulation, the radar will see a string of 16 alternating logical 1's and 0's with a double 1 to bookend the stream. An example of this could would look like equation 2.1. While a bird is in flight and in range of a WSR-88d, the radar will see these exact strings in the data. The process of tracking these birds involves watching the unique reflection patterns change range gate for moving towards or away from the radar, or the reflections will appear to move in azimuth angle as the bird circles the radar.

$$0101010101010101 - 1 - 0101010101010101 - 1 - ... \tag{2.1}$$

In future work, additional switches with unique impedances can be added to provide a larger range of backscatter amplitudes for more logical numbers. By specifically choosing different impedances, there is a power differences in the reflections from pulse to pulse and it is then possible to have multi-bit codes. An example of a 4 switch code can be seen in equation 2.2.

$$0123412341234 - 0123412341234 - ... \tag{2.2}$$

It follows that by choosing different orders of impedances and pairing them with the current 16 bit counter on the tag, there is a wide variety of potential codes to encode on individual tags by simply changing combination of the impedances and their associated counter values.

The goal of the proposed system is to operate the same as a standard hybrid passive-active RFID tag, but at 2.85 GHz and a prf range of 300 Hz to 1.3 KHz. To properly illustrate this, full backscatter capabilities should be verified via testing at these parameters. The system should demonstrate an ability to recognize an incoming WSR-88D pulse, rectify the pulse so that the wave triggers the digital logic section, and modulate the switch. By modulating the incoming pulses across known impedances, a unique signature can be encoded according to a chosen modulation scheme. Measurements should illustrate the ability to backscatter modulate multiple patterns, as well as, the ability to backscatter modulate at multiple power levels, and the ability to back scatter across a the NEXRAD prf range.

The proposed RFID tag should be capable of receiving and modulating signals as low as -10 dBm. This level of sensitivity allows for the proposed system to achieve the desired range of 10 km with reasonable conditions. For the system to show an ideal ASK modulation scheme, a modulation factor, M, of 0.25 should be measured. Reasonably, a lower modulation factor can be attained, and the system is still capable of encoding the pulses through ASK.

2.3 Link Budget

The Friis radio link formula can be broken down into a simple form for calculating the power received by a radio antenna. Through breaking down all the variables into decibel units terms, simple addition and subtraction can be used to calculate the total power received in decibels. By taking the transmitted power and subtracting losses incurred along the path from transmitter to target and adding for the gain of the transmitting and receiving apertures we can see the total power received. Pozar re configures the Friis equation as seen in equation 2.7[20]. This form of the equation is a general form and is useful in any application, but an RFID specific version has been created by Durgin that allows for easy accountability of all of the unique losses and challenges associated with RFID and backscatter specific radio communication.

When describing an antenna, it is important to clarify in the discussion whether directivity, gain, or realized gain is being used. While directivity is a figure of merit and can give an idea on the performance of the antenna in a particular direction, it does not give a proper estimation of the antenna as a radiator in a specific direction. The gain of an antenna gives a value to properly describe the performance of an

antenna, or how efficient it is at radiating in a desired direction. The gain of an antenna is defined as "the ratio of the power gain in a given direction to the power gain of a reference antenna in its referenced direction"[21]. However, the gain of an antenna does not fully detail the characteristics of the antenna chain and account for the losses in the transmission chain. For a proper measurement, the realized gain of the antenna is used. In the Friis transmission equation and its derivatives, the gains associated with the system are the realized gains of each device. The realized gain accounts for the directivity,$D(\Theta, \Phi)$, radiation efficiency, η_{rad}, and reflection mismatches, η_r, in the transmission line as seen in Equation 2.3. The realized gain is the multiplication of the directivity of the antenna multiplied by the antenna's radiation efficiency and the associated losses associated with the antenna. By using the realized gain, there is one variable that accounts for the total maximum gain of the system in a specific direction[21].

Realized gain is defined:

$$G_{RG} = \eta_r \eta_{rad} D(\Theta, \Phi) \tag{2.3}$$

η_r is defined as:

$$\eta_r = (1 - |\Gamma|^2) \tag{2.4}$$

Γ is defined as:

$$\Gamma = \frac{Z_{antenna} - Z_{generatorload}}{Z_{antenna} + Z_{generatorload}} \tag{2.5}$$

and η_{rad} is defined as:

$$\eta_{rad} = \frac{R_{rad}}{R_{rad} + R_{loss}} \tag{2.6}$$

As described in detail by Durgin, the Friis equation can also be broken down to an RFID specific form as seen in equation 2.9. He stated that backscatter radio is fundamentally different from conventional radio communication and that the Friis equation needs to be compensated as such. Due to the passive nature of these backscatter RFID tags, it is important to note the limits, associated losses, and other factors when detailing the link budget for an RFID system. Durgin describes four different link budgets to fully characterize passive RFID networks. Two of his derived equations are essential to this study and provide the theoretical basis that long range RFID is possible. Durgin's link budget equations are similar in function to the classic link budget equation, but have been broken down to directly plug in the characteristics of the transmitter and RFID tag. Durgin's monostatic backscatter is seen in equation 2.9 and is more applicable for this study's purpose. It should be noted that several of the losses associated with Durgin's form vary from case to case. The path loss and clear sight losses are minimal in this study's application when compared to classic applications where there are objects and potentially walls between the transmitter and RFID tags[11].

Pozar's Friis equation is defined as:

$$P_r(dBm) = P_t - L_t + G_t - L_0 - L_a + G_r - L_r \tag{2.7}$$

In equation 2.7 path loss is accounted for as a source of loss for the entire system. Path Loss is defined in this equation as:

$$L_0(dB) = 20log(\frac{4\pi R}{\lambda}) > 0 \tag{2.8}$$

Durgin's Monostatic Backscatter link budget is defined as:

$$P_R(dBm) = \frac{P_t G_{TR}^2 G_t \lambda^4 X^2 M}{(4\pi r)^4 \Theta^2 B^2 F_2} \tag{2.9}$$

Table 2.1: Link Budget description

Transmit power (kW)	P_t	700
Transmit/Receiver antenna gain (dBm)	G_{TR}	45.5
RFID antenna gain (dBm)	G_t	-2
Lambda	λ	0.1053
Polarization Mismatch	X	0.5
Modulation Factor	M	0.25
Range (km)	r	80.96
On-object gain penalty	Θ	Calculated in Tag's gain
Path blockage loss	B	Negligible, direct sight line
One-way power-up fade margin	F_2	Negligible, direct sight line

In order to calculate the power directly received one-way by the RFID tag the Friis equation needs to be rearranged again; however, it is already derived by Durgin. Durgin's Power-Up link budget is defined as:

$$P_R(dBm) = \frac{P_t G_{TR} G_t \lambda^2 X \tau}{(4\pi r)^2 \Theta^2 B F} \tag{2.10}$$

Where τ is the power-transmission coefficient.

The final factor to take into account is modulation factor (M)[22]. The proposed tag has two states, they are when the tag is absorbing or reflecting, the modulation factor corresponds to the reflection coefficient of two states as seen in equation 2.11. These two states are made by modulating the switch between a two impedances as discussed in chapter 1. By breaking down the Friis equation and substituting in

the mismatch due to the modulation circuitry, the expected power received by the radar can correctly be calculated. Typically, M = 0.25 is commonly used for ASK modulation schemes[11].

$$M = \frac{1}{4}|\Gamma_A - \Gamma_B|^2 \tag{2.11}$$

The WSR-88D has a minimum power detected level of -113 dBm and the proposed tag has a minimum power detected level of -10 dBm due to the envelope detector's restrictions. However, the WSR-88d is the limiting factor in the total range calculations of this design. Since the signal has to bounce off the tag and travel back to the radar, the power received is severely limited by the total range. Both of these minimum signal strengths are used in the calculations to determine the maximum range of the system.

In order to determine the total operating range of the proposed tag, Durgin's equation was used to calculate the minimum range with these variables. By plugging into Durgin's equation that range equals 72 km, polarization mismatch is 0.5, 0 dB of gain for the RFID antenna, and -2 dB of additional losses it can be seen that the total power received is -113.96 dBm back to the radar after modulation. These variables were chosen as an example of some of the worst conditions the system can be operating with and provides a floor of expected range.

The maximum range that can be achieved is based upon the lowest amount of power the WSR-88d can detect and can also be calculated using equation 2.9. With using 0 dB for losses, 0 dB of gain for the RFID tag, and no polarization mismatch, the maximum range expected is 121 km. This calculation establishes the absolute ceiling of expected range by the proposed system under ideal conditions.

For a conservative estimate of the system's performance, with 0.75 polarization mismatch, a modulation factor of 0.25, -2 dB of losses, and 0 dB of gain the system achieves 83 km of operable range. Potentially, with future improvements to the RFID tag consisting of an antenna with more than 0 dBi of gain this operable range could be stretched to 100 km and above.

2.4 System overview and explanation

The proposed tag for this study mimics that of a standard RFID tag in the UHF range[14]. Notably, the design uses the antenna as a 1-port network for both receiving and backscattering. A high speed reflective RF switch in parallel with the digital logic provides backs scatter capabilities for the tag. This is achieved by alternating between the reflective state with the closed switch and the absorbing state with the opened switch that is connected to a shorted transmission line to ground with a specified load impedance. Two positives to working in this configuration is that the design allows the digital logic to receive every pulse from the WSR-88D providing a constant interrogation of the RFID tag and to also maximize power efficiency by using reflective switches. Due to the system being able to observe every pulse from the WSR-88d, the tag operates by triggering off the falling edge of the previous pulse, the system then backscatters the next pulse with the desired impedance via the switch.

Standard operating passive RFID tags utilize the power transmitted by the transmitter for backscatter and do not require an additional power source. For this design, the tag will operate similarly to a passive RFID tag with the pulse activating the digital logic integrated chips, but the system will have a battery to operate the

switches for the particular backscatter pattern. The design is capable of providing a functional ASK, PSK and potentially a Quadrature amplitude modulation (QAM) modulation patterns. Due to the inclusion of a battery, the proposed tag has access to this wide set of modulation schemes, as well as, long range detection, and a high data quality. The inclusion of the battery also comes with negatives. Batteries increase the initial and recurring costs of the tags, total tag weight increases, and there is a temporary life span for each individual tag that passive tags do not have. Truly passive tags work only off the energy absorbed by the incoming RF pulse, they do not need an additional power source to function. This leads to passive tags being very small in form factor and light weight due to only need transistor level logic and microstrip lines to function in the final surface mount component design. For this design, a compromise must be made between functionality, lifespan, and total weight. With birds carrying these tags, a threshold must be put in to place for the maximum allowed weight.

2.4.1 Modulation Scheme Examples

The proposed tag operates off of a singular switch providing the chosen modulation schemes. From the switch being a commercially available version, the impedance

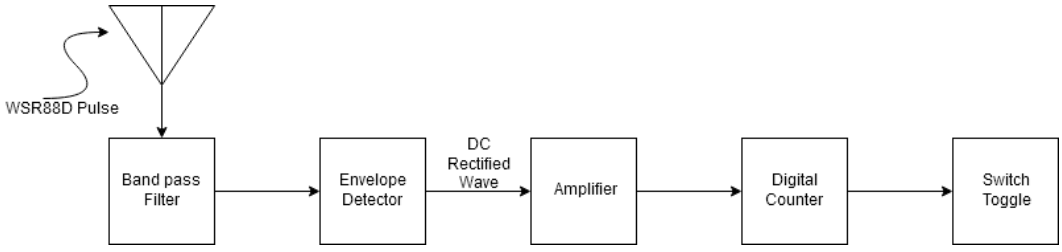

Figure 2.1: A block diagram of the proposed system's function.

is predetermined and can not be changed. For this study, only the terminated impedance was changed. A variety of impedances were chosen to demonstrate different the effects on the measured backscatter. Future work includes addition of QAM backscatter modulation as mentioned previously before. By using transmission line theory the impedance of the switch(es) in parallel with the envelope detector, the total impedance of the system can be calculated. By taking this impedance and adding a phase shift classic QAM modulation can be achieved centered around the center of the smith chart. For the proposed system this can be seen in figure 2.6.

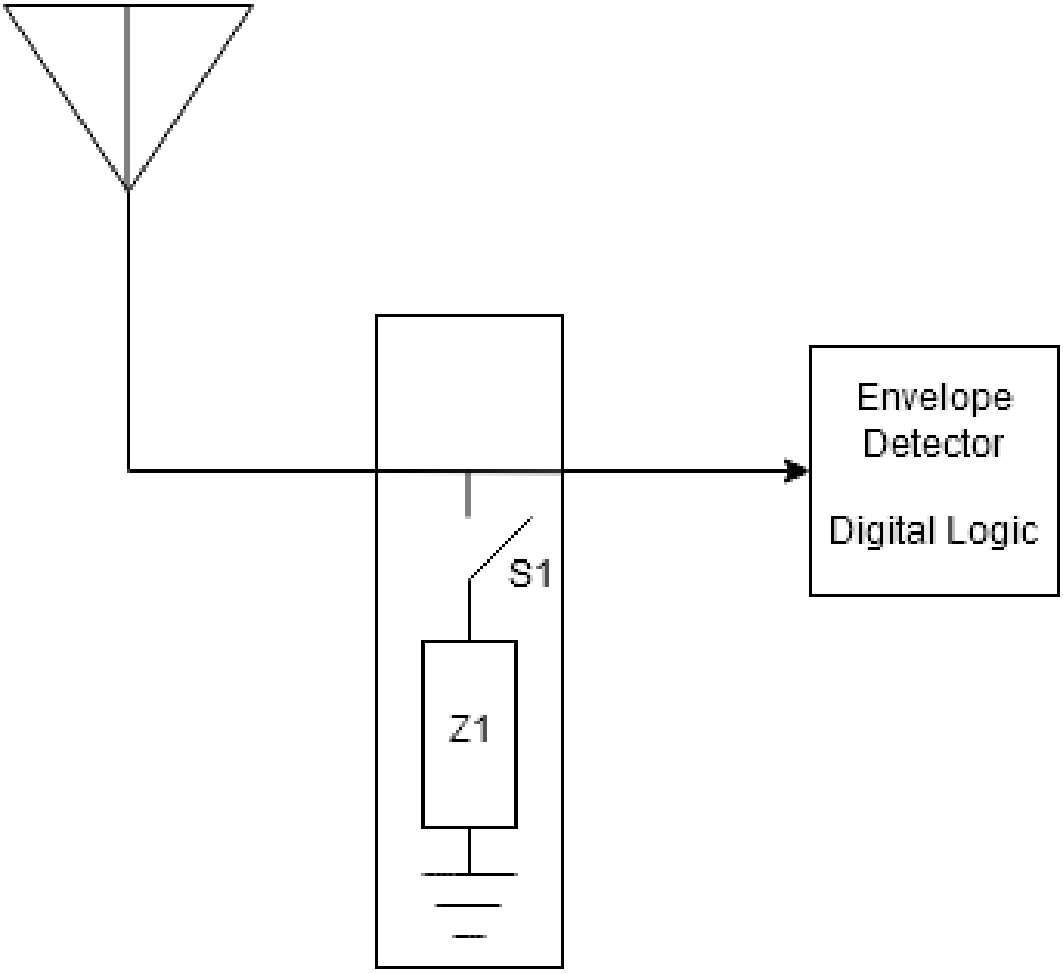

Figure 2.2: A block diagram example of impedance modulation.

As seen in figure 2.3, the proposed tag has been expanded to a setup with four different impedance and switch combinations. The system would function similar to the tested single impedance system, but different levels of backscatter can be achieved by each impedance being unique. An example of this configuration is used still requires the proposed tag to operate by receiving an incoming RF wave, rectifying it through an envelope detector, and triggering the counter. From the counter's output, each switch is individually turned on and off in a typical 4 bit

counter pattern as seen in table 2.2. By choosing 4 different impedances, up to 24 unique combinations can be used per device if desired when using the full capabilities of a 4 bit counter. Commonly, 2 bits are used to create the 4 common QAM reflections as seen in figure 2.5[14]. An example of the proposed tag showing basic PSK functionality can be seen in figure 2.6. The impedance of the RFID tag was calculated, then a phase shifted version was set as the load impedance of the switch to create this modulation scheme. In chapter 5, different impedances have been selected to show the difference in the total power backscattered by the tag.

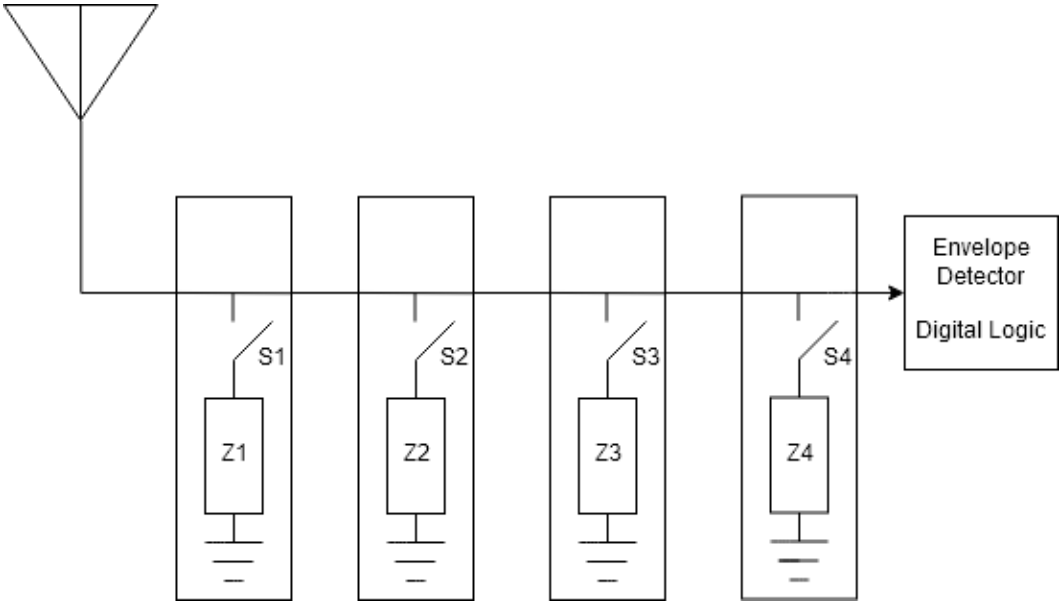

Figure 2.3: A block diagram example of impedance modulation via four different impedances.

Counter	S1	S2	S3	S4
0	0	0	0	0
1	0	0	0	1
2	0	0	1	0
3	0	0	1	1
4	0	1	0	0
5	0	1	0	1
6	0	1	1	0
7	0	1	1	1
8	1	0	0	0
9	1	0	0	1
10	1	0	1	0
11	1	0	1	1
12	1	1	0	0
13	1	1	0	1
14	1	1	1	0
15	1	1	1	1

Table 2.2: An example of a 4-bit counter logic table

The digital counter used in this study is a standard 4 bit counter made with j-k flip-flops. The incoming clock pulse triggers the flip flops and the system counts up 1 bit at a time. This produces the values seen in table 2.2

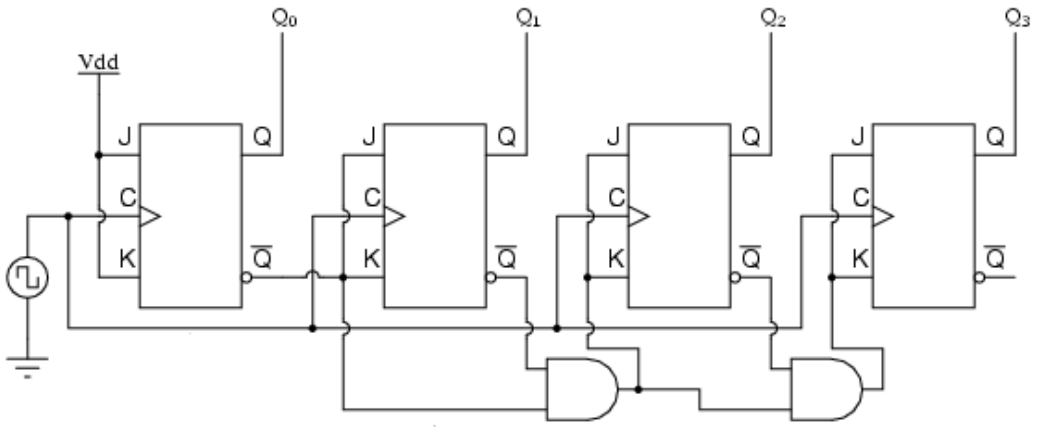

Figure 2.4: Example of a standard 4 bit counter made from j-k flip-flops[23].

By placing the switches in parallel and with very short stubs connecting them to the transmission line, negligible power is lost even by having multiple stubs in the pathway to the envelope detector. The overall design is highly power efficient for making sure every pulse is received by the logic portion. By triggering on the falling edge, entire pulses are seen by the tag before the next pulse is properly reflected back to the WSR-88d.

The Smith chart in figure 2.5 demonstrates QAM modulation across the entire NEXRAD frequency band of 2.7 GHz to 3.0 GHz. With minimal change in the phase and impedance displayed across the frequency band. The impedances used are in table 2.3. These impedances were simulated in AWR as an example of potential modulations that could be built by diode based switches instead of using commercially available switches with pre chosen impedances.

Color	Impedance	Phase
Brown	20.51 Ohms	60.82
Red	107.55 Ohms	60.82
Pink	20.51 Ohms	-60.82
Blue	107.55 Ohms	-60.82

Table 2.3: Associated impedances simulated in AWR for QAM modulation.

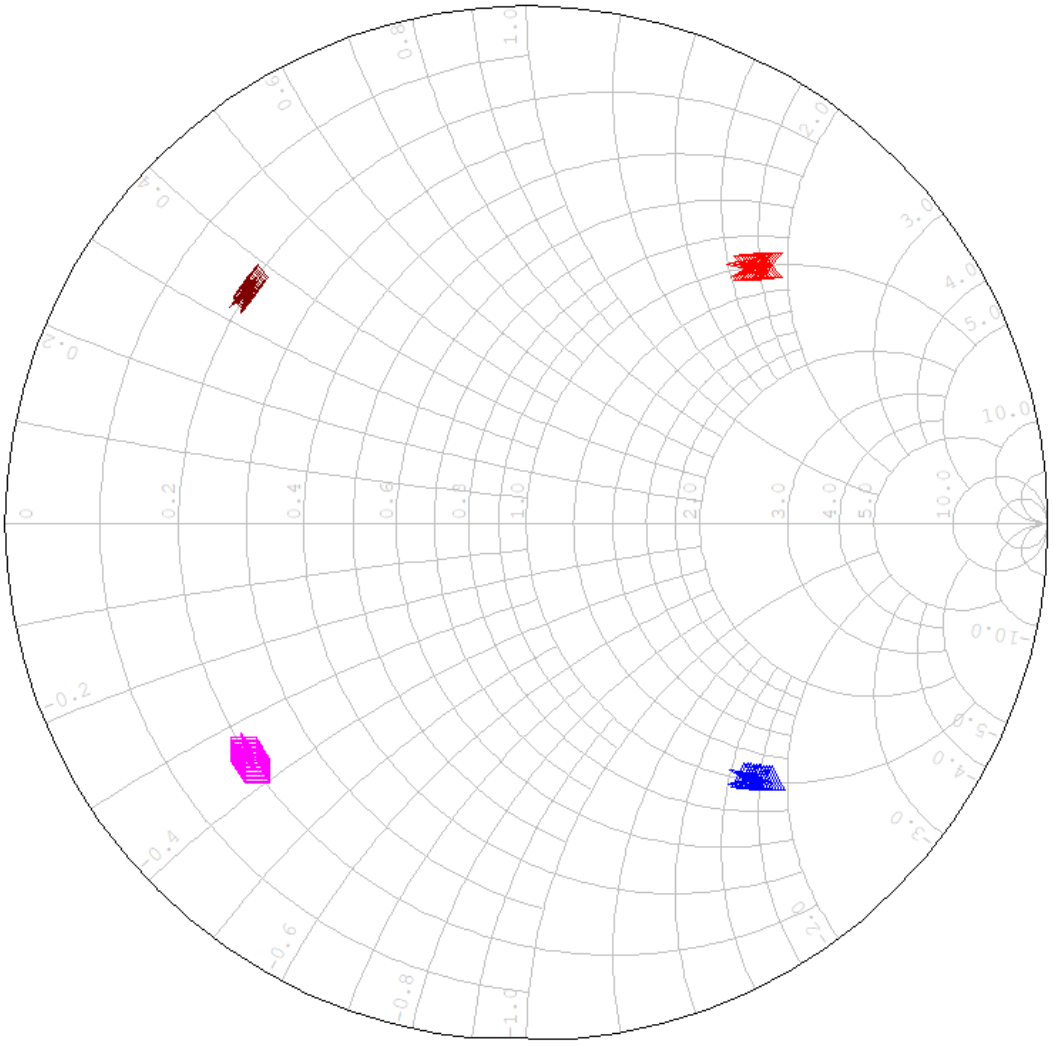

Figure 2.5: Example of standard QAM modulation via 4 different impedances.

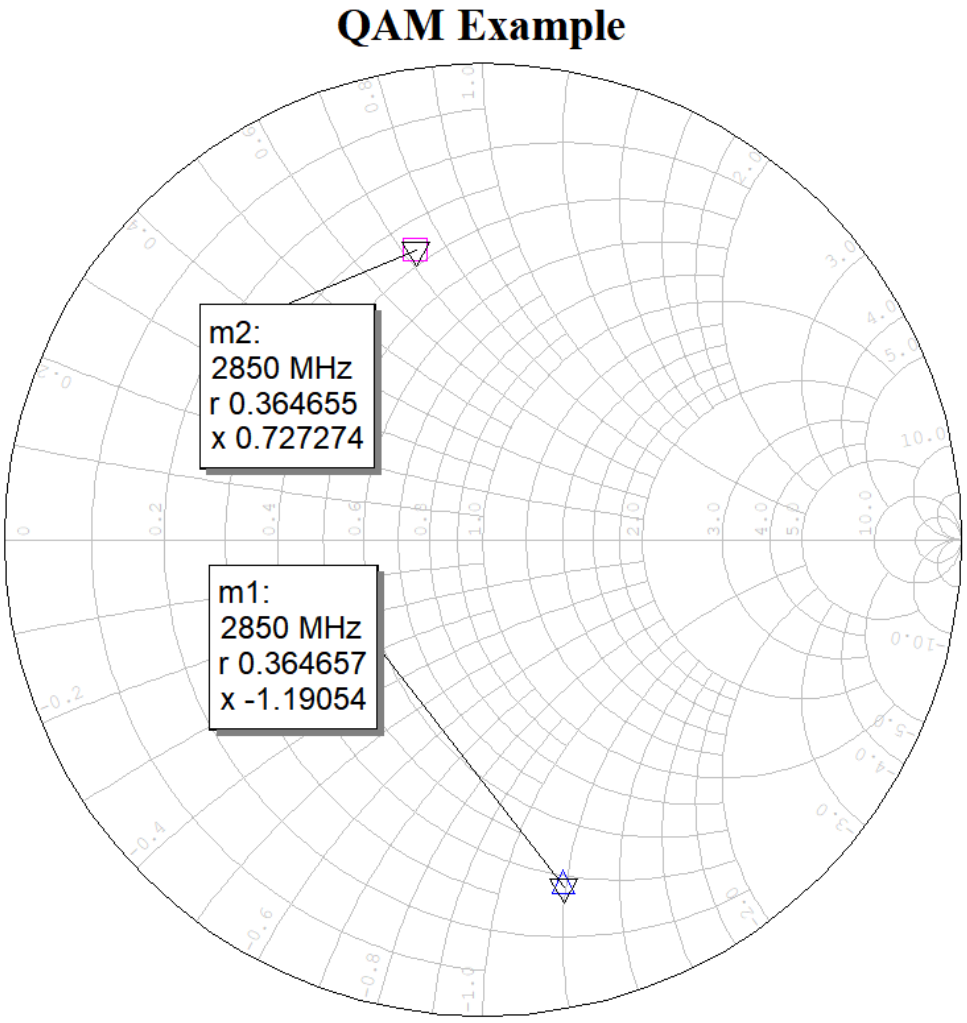

Figure 2.6: QAM modulation with the system's impedance and a phase shifted impedance.

2.5 Conclusion

The goal of this study is to recreate common RFID technology at a different frequency band and to integrate the RFID tag with an established radar network. In principle, the tag will function almost identically to other RFID tags used at standard RFID frequencies. This chapter has detailed how the proposed RFID tag is capable of implementing common modulation schemes used across a variety of technologies and how the radar interacts at a higher level with the proposed tag. This chapter has also showcased the total maximum and minimum range achievable by the proposed tag and how these values were calculated. For these calculations, considerations were made to consider a variety of conditions to emulate a non ideal tag. Overall, an analysis of the proposed system was done by examining the link budget, overall power requirements, and briefly introducing the trade offs associated with designing the proposed tag[14].

Chapter 3

Components of proposed tags

3.1 Introduction

The other requirement for this study was to check the viability of using commercially available parts for mass production of the proposed tag if the tag meets the design goals of this study. This chapter details the parts used and the associated trade offs with these commercially available parts. In the conclusion, suggestions are made on how to enhance the performance of the system and potentially expand the maximum range. The front end of the proposed RFID tag is composed of a typical ceramic prepackaged antenna from Johanson and a prepackaged ceramic bandpass filter from Mini-Circuits. The combination of these 50 ohm matched devices provides an efficient communication channel for the tag with low total loss. Additionally, these ceramic parts are cheap, efficient, and temperature resistant.

3.2 Antenna

The selected antenna from Johanson Technology fulfilled all the minimum requirements for this project. The antenna has a 0-2 dBi gain while maintaining a form

factor that is perfect for using in a small RFID tag. The antenna also benefits from being temperature resistant. With the tags being taken into high altitude, the antenna will be exposed to lower temperatures and needs to maintain its characteristics across the wide range of temperatures it will be exposed to. The antenna has a measured return loss of 9.5 dB. As mentioned, the form factor of the antenna is very small the overall size is 8mm long by 1mm tall and 1mm wide. As it is prepackaged, it is easily matched to 50Ω at 2.85 GHz. The final fabricated design was made in house and the antenna was placed on a Rogers 4350B 30 mil board. A small microstrip line was required to properly match the antenna to 50Ω as can be seen realized in figure 3.3. Finally, due to the antenna's design it is very efficient from 2.3 GHz to 2.9 GHz, but capable of going all the way up to 3.0 GHz to detect larger pulses. Overall, the antenna was the weakest part of the design. Being severely limited by choosing between commercially available antennas required a sub optimal choices. A better antenna for this design would be made to match with the WSR-88d's frequency band while maintaining a small form factor and providing the maximum gain to size ration achievable. Through S11 analysis, the antenna has been calculated to have an impedance of 24.65+j3.15.

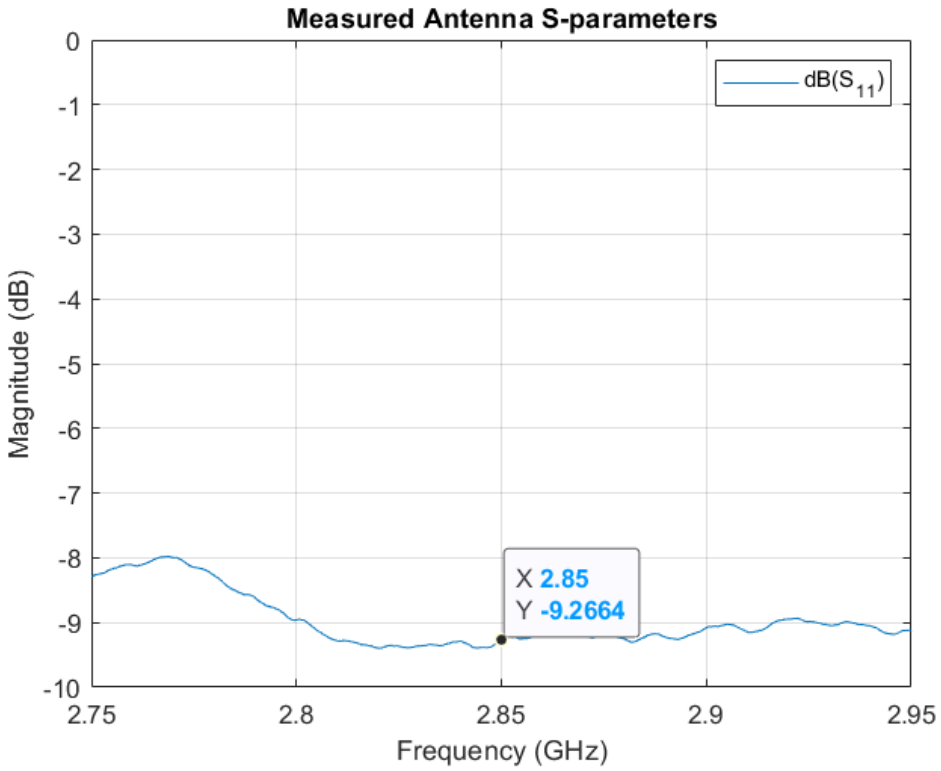

Figure 3.1: S-parameters of the 2600AT44A0600 Antenna.

As seen in figure 3.1, the antenna operates stably across the entire frequency band. The reflection coefficient, S11, of the antenna is roughly -9 dB and lower through the entire band. The antenna shows 100 MHz of bandwidth across the frequency band.

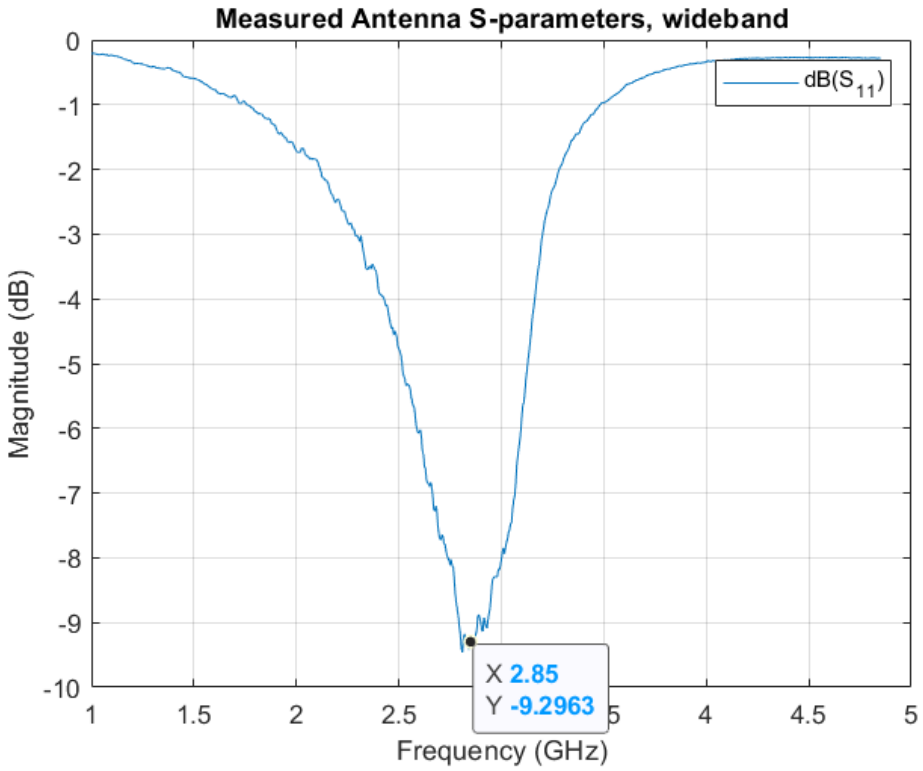

Figure 3.2: Wideband sweet of the S-parameters of the 2600AT44A0600 Antenna.

As seen in figure 3.2, the antenna is matched very well for 2.85 Ghz, and an effective bandwidth of around 2.3 GHz to 3.2 GHz. The antenna shows around 90 percent efficiency in the NEXRAD's frequency band.

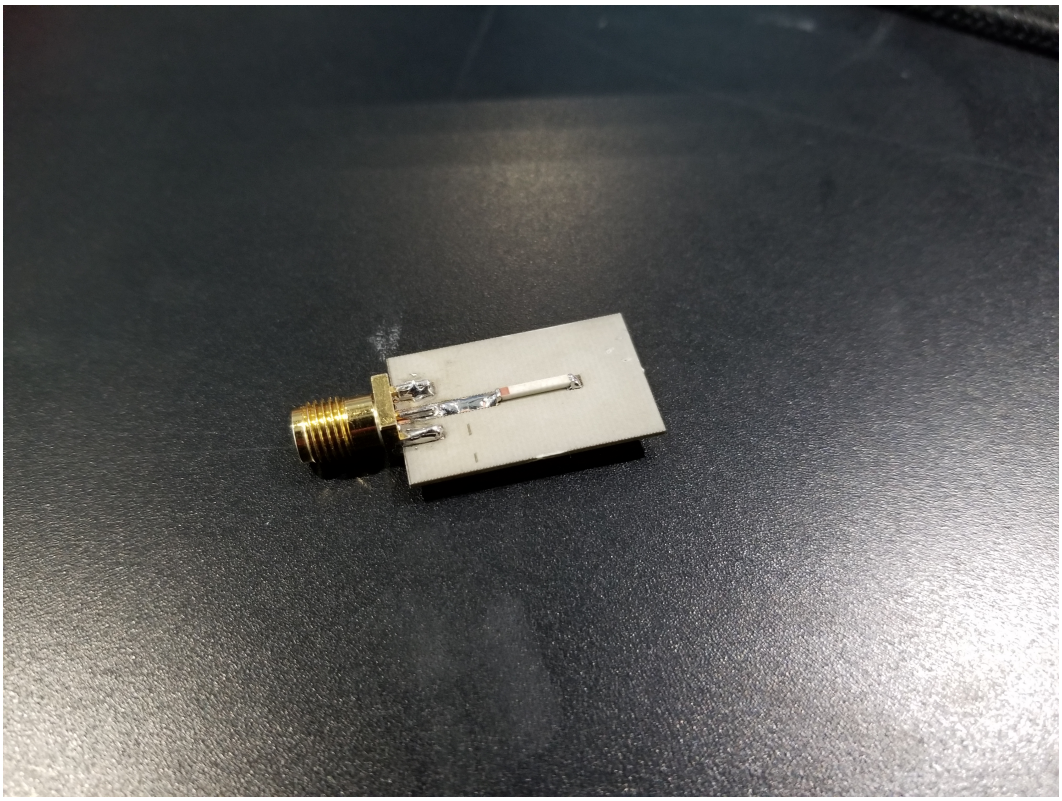

Figure 3.3: Assembled prototype of the 2600AT44A0600 Antenna.

In figure 3.3 the assembled antenna can be seen. The antenna was mounted on a 30-mil Rogers 4350B board. The board was laser etched via an LPKF laser ablation machine by subtractive manufacturing. The design for the matching network was created in Ansys HFSS according to specifications from Johanson and then converted to an LPKF drilling file to be manufactured. A microstrip matching network was designed in AWR. Several considerations were made in the matching of the antenna. Due to minimal performance differences between an LC network and a microstrip line, a microstrip line was chosen. This design provided an S11 of -18.74 dB in AWR simulations over a lumped components matching network that provided an S11 of -23.82 dB as seen in figure 3.4. For both fabrication and logistic

reasons, the microstrip was a more viable option for initial tests, but it should be noted there is room for improvement in future considerations. The antenna matching was done via an National Instruments AWR solving simulation. The simulation was used to find the possible solutions for maximum matching of each type of matching network.

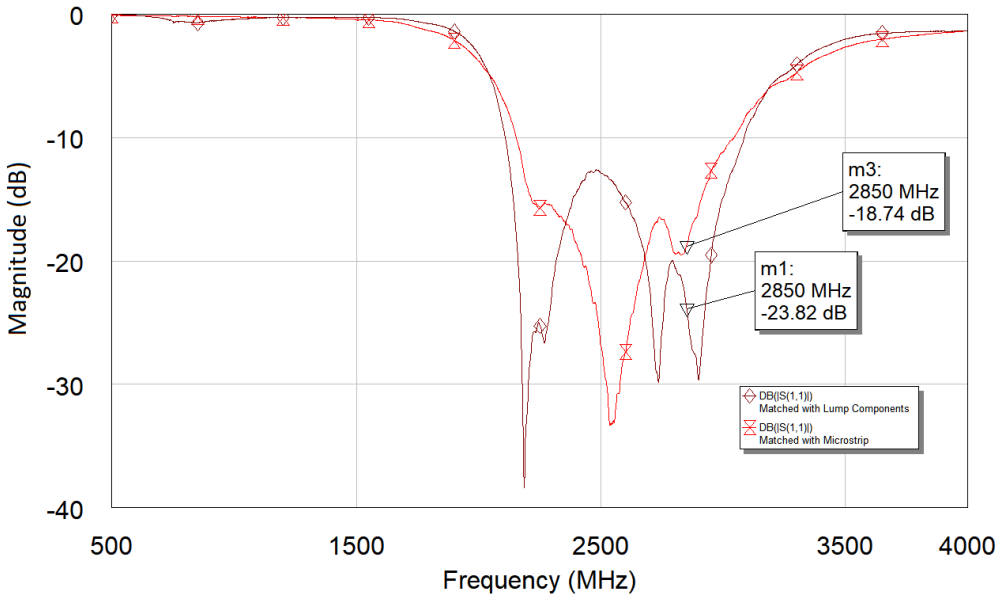

Figure 3.4: AWR Simulation of matching network performance

3.3 Bandpass Filter

The bandpass filter was ultimately selected because the form factor and quality was impossible to beat in house and fit the requirements completely. The center frequency is perfectly matched at 2.85 GHz with 100 MHz of bandwidth. Additionally at 2.85 GHz the filter has an insertion loss less than 4 dB and a VSWR of

1.3. As mentioned with the antenna, small, ceramic designs are optimal for this application and have good temperature resistance when looking at performance. In figure 3.5 we see the S11 is -15.467 dB at 2.85 GHz and the S21 is -1.843 dB at 2.85 GHz with the -3 dB cutoff points at 2.66 GHz and 3.08 GHz. Overall, the filter has good performance and outperformed simulations for in house fabrication methods that are able to be fabricated at the Radar Innovations Laboratory. Additionally, this prepackaged option also is a great choice because of in house limitations on form factor friendly designs. The ceramic surface mount filter is marginally smaller and more compact than the Radar lab's capabilities as a fabrication house. Due to the current technology available, the Radar lab is not capable of fabricating ceramic devices. The characteristics of the filter line up very well with the requirements for detecting only WSR-88d pulses. The chosen bandpass filter was an optimal choice for the proposed tag and can be kept in the final product.

3.4 Load Impedances

A critical part of this design is the design of the terminated loads for the switches. These impedances determine how much energy is backscattered and are used to create the desired amount of difference between reflected and absorbed pulses. For simple testing purposes with readily available SMA terminations, 50 Ohms and 88 Ohms were used to demonstrate basic functionality of the system. For future designs, the impedance of the system was calculated and phase shifted to allow for QAM modulation as seen in chapter 2. As seen in figure 3.6 and figure 3.7, purely real impedances that are closely matched to the system do not provide a large difference in the plotted impedance. When optimizing modulation schemes,

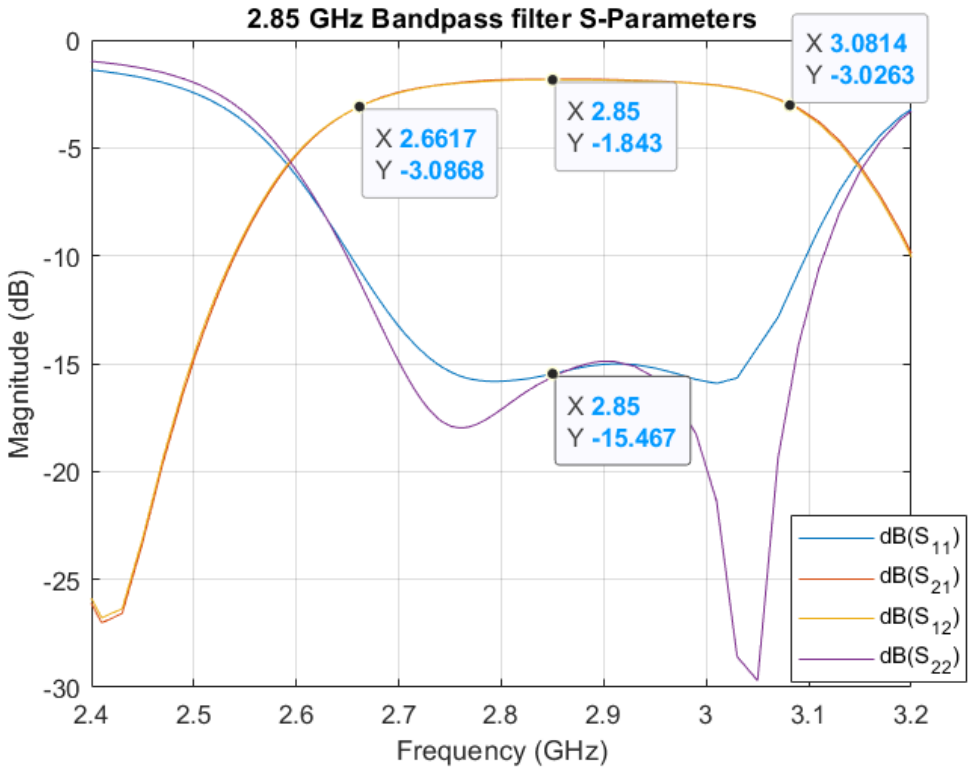

Figure 3.5: S-parameters of the 2.85 GHz bandpass filter

non-matched impedances can be chosen to maximize the difference in returns as was see in figure 2.6. In chapter 5, the corresponding backscatter graphs can be seen that illustrate the difference between the 50 and 88 Ohm impedances.

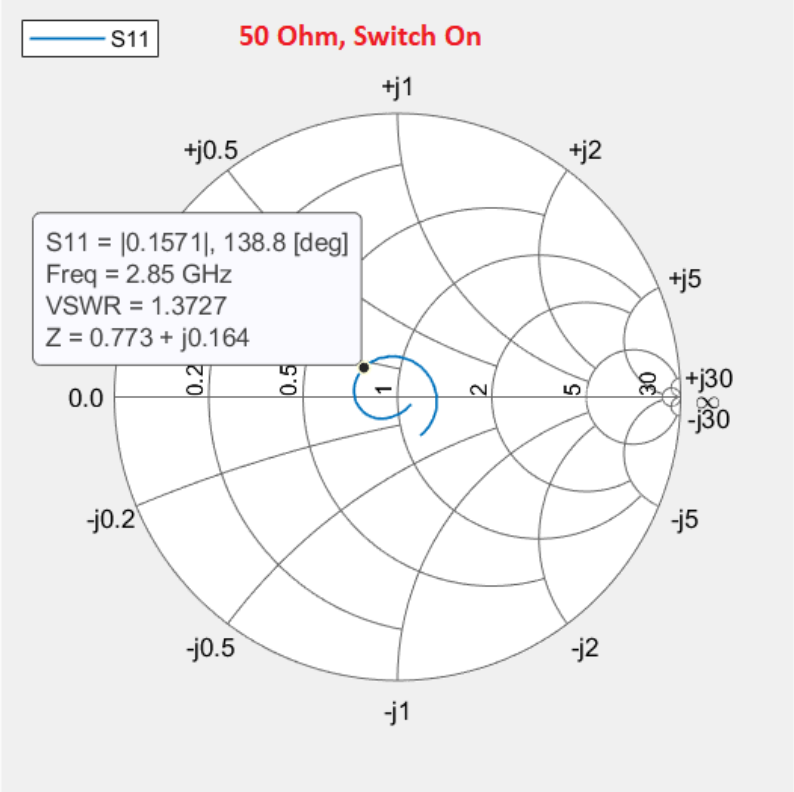

Figure 3.6: Smith chart plot of 50Ω termination on system

3.5 Backscatter with the front-end components

With the desired operation to function like a passive tag, the chosen components were selected with this in mind and there are not any compatibility issues between the front end components. Since the switches naturally reflect power due to impedance mismatch, the frequency is not changed and the signal passes through the bandpass filter again, this time in the opposite direction. It is then radiated out of the antenna to be detected by the next pulse from the radar[14], [16]. The biggest trade off of having the bandpass filter to narrow down the RFID tag's acceptance to only WSR-88d's pulses is dealing with double the loss through the signal traveling

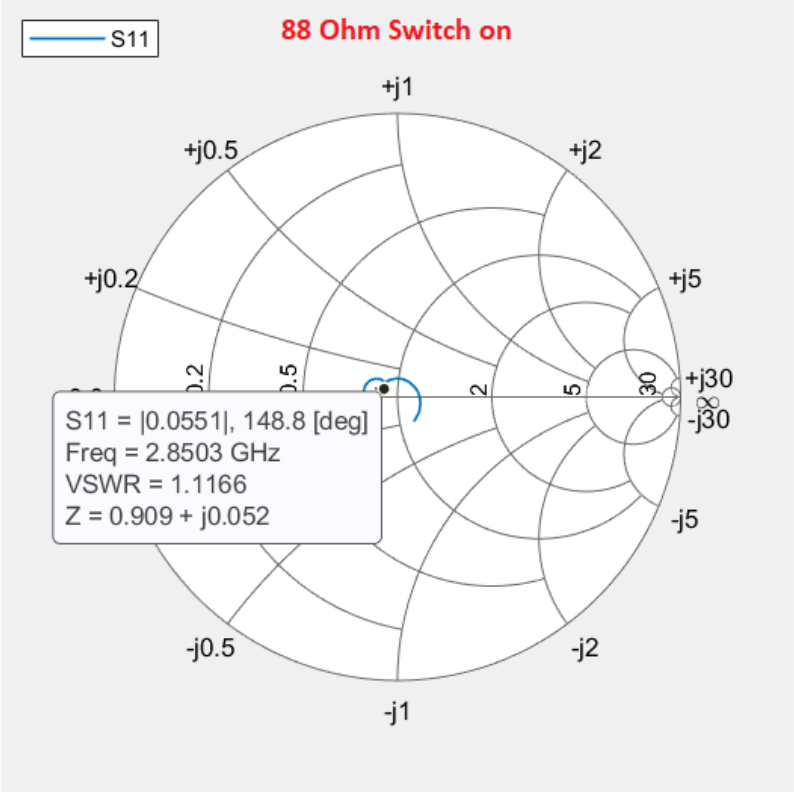

Figure 3.7: Smith chart plot of 88Ω termination on system

twice through the filter. Due to the nature of the antenna naturally being designed wide band from 2.3 to 2.9 GHz, the filter is required to not pick up errant radar pulses down in the cellular and wifi ranges.

3.6 Switch

The chosen switch for this design is a reflective open switch by Analog Devices. The switch was chosen for its low insertion loss and high return loss at 2.85 GHz. Additionally, the switch is very low power and is ideal for a battery operated devices. By minimizing the losses associated with the switch, the maximum amount

of power can be reflected for backscattering purposes or the minimum amount of power can be incidentally reflected when the tag is in absorbing mode if desired. Baseline testing of the switches was done on a large frequency sweep to determine how the S-parameters act at a range of frequencies.

The switch was tested for its S-parameters by testing across a frequency sweep to determine if modulation could be done properly at across the entire NEXRAD frequency band. Figure 3.8 and figure 3.9 shows that a constant -20 dB S_{11} was achieved while the switch was on and terminating into a 50 Ohm load and -1.5 dB S_{11} was achieved while the switch was reflecting. The switch performs well across the entire frequency band and has a minuscule difference in S-parameters across the frequency sweep. This steady performance helps provide stable modulation from pulse to pulse at all potential frequencies.

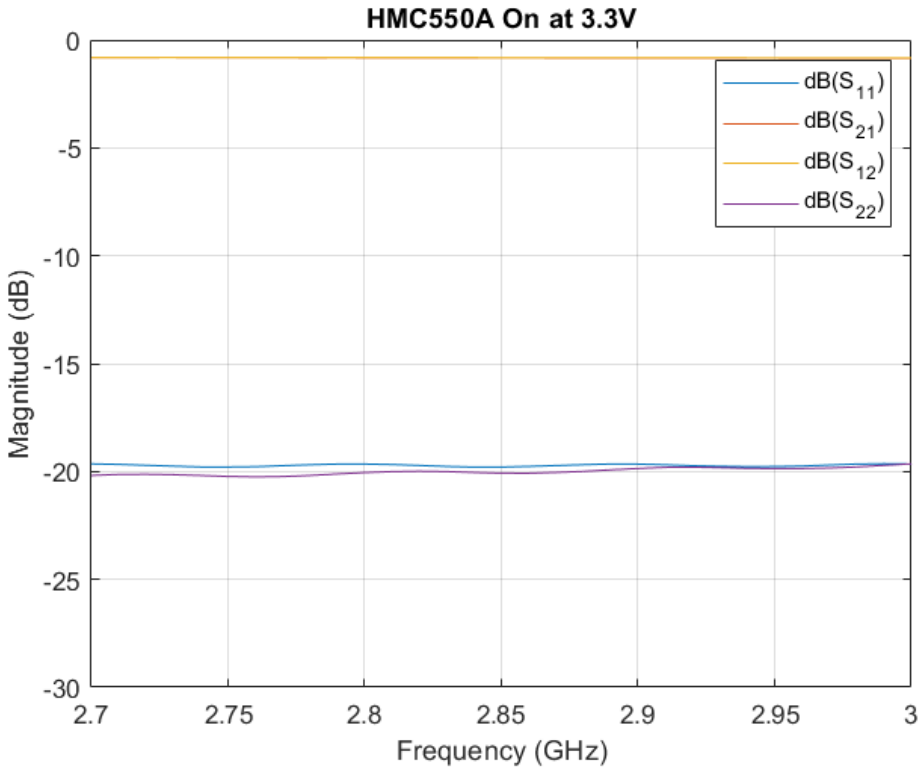

Figure 3.8: S-parameters of the HMC550A powered On.

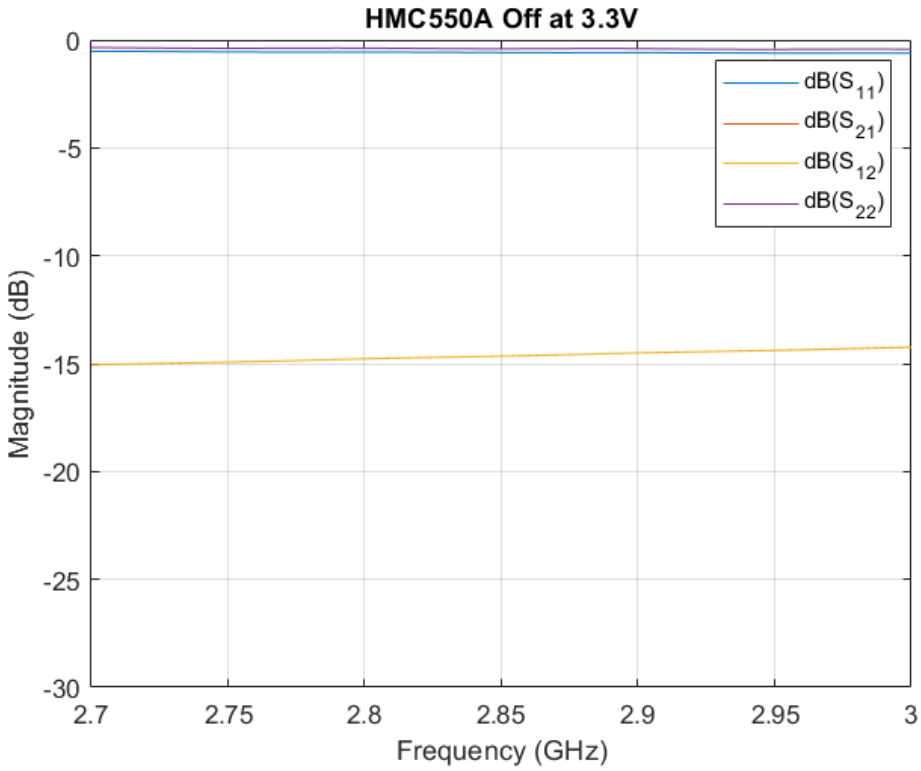

Figure 3.9: S-parameters of the HMC550A powered Off.

3.7 Combination of parts and expected attitude

Figure 3.10 of the proposed RFID tag shows a typical RFID design. The parts internally use high speed RF diodes to operate as switches and for the envelope detector. Every part has been selected with the 2.85 GHz frequency in mind. In the current form comprised of SMA connected pieces, there is an expectation of some additional losses that would smaller with transmission line connections in the final design.

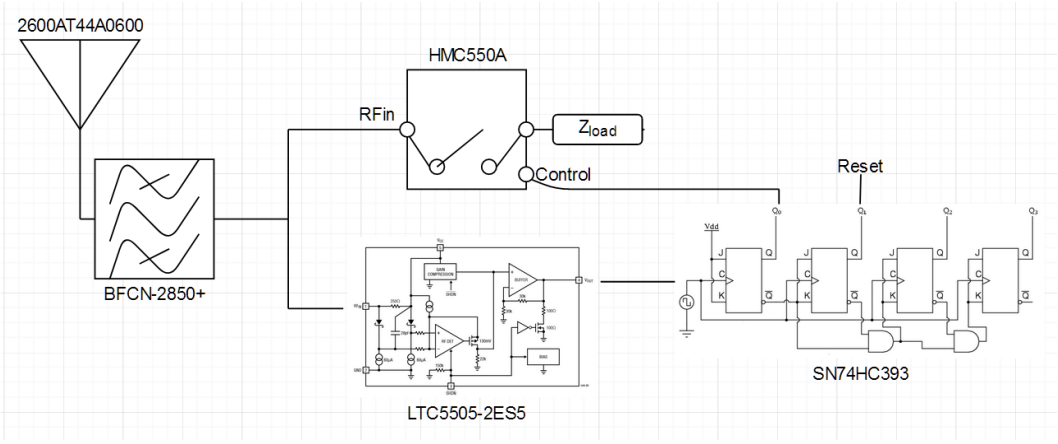

Figure 3.10: Circuit level schematic of the proposed RFID tag

A transmission line analysis of the proposed RFID tag was done to identify the impedance of each individual part. Through knowing the impedances involved with each part, the total impedance of the system can be calculated. When configuring the system for different modulation schemes, a different predetermined system impedance is chosen for each mode. In order to achieve this desired system impedance, the switch's load impedance must be calculated for. As seen in chapter 6, the correct impedance for QAM modulation was calculated and simulated. Figure 3.11 shows how the system was broken into transmission line segments.

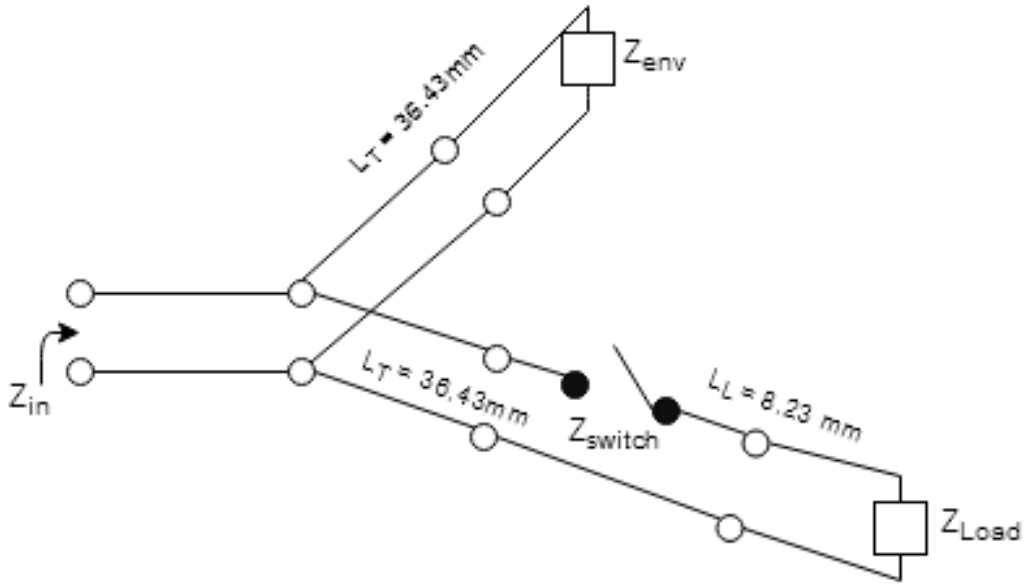

Figure 3.11: Transmission line analysis of the proposed RFID tag

The following values in table 3.11 were calculated by measuring each part's S11 on a network analyzer at 2.85 GHz. The load impedance does not have a listed value due to the nature of the system. The load is chosen after a knowledge of the system is gained and the desired modulation scheme is selected. For the proposed system a load of 50Ω and 88Ω was used to demonstrate modulation schemes.

System part	Impedance
Envelope Detector (Z_{env})	100.8-j30.15
Switch (Z_{switch})	10.45+j71.75
System State One (Z_{state1})	23.4+j36.97
Characteristic Impedance Z_0	50
Load (Z_{load})	Varies

Table 3.1: True Impedance Values of each part

As mentioned in chapter 2, once the impedances of the system and antenna are known, the modulation factor of the system can be calculated. With the current proposed antenna being used as the Z_{ant} value, the system achieves a modulation factor of 0.1013. This modulation factor was calculated using the 50Ω termination as the switch's load impedance. In future work, the modulation factor can be improved to the ASK standard of 0.25.

3.7.1 Navigating the Smith chart with selected impedances

For the design of this system's modulation scheme, as seen via the Smith chart response of each stage, the load impedance was calculated to be 180° around the center of 50Ω away in phase from the reflecting stage's load impedance, or a quarter-wave length. In order to calculate the reflecting stage of the proposed RFID tag, each part's input impedance was measured individually. The initial impedance values in table 3.1 were calculated as seen through the transmission lines by measuring each impedance through a spectrum analyzer. Since the impedance of the system in the open switch, reflecting stage does not change due to the impedance of the switch and envelope detector being predefined, the impedance of the closed switch, terminated load stage must be changed. The open switch, reflecting stage's impedance is comprised of the switch and envelope detector's impedance being placed in parallel with 36.43 mm long transmission lines connecting them to a 3 dB power splitter. The closed switch, terminated load stage's impedance is comprised of the envelope detector connected via a 36.43 mm transmission line length being placed in parallel with a 44.66 mm long transmission line attached to a user defined load impedance.

With the total system impedance being known, a load impedance can be chosen

for the system to still have the same magnitude as when the switch is closed, but the impedance is phase shifted. In this case, the desired phase shift was selected to make the impedance be located on the exact opposite corresponding location of the Smith chart as seen in figure 2.6.

To determine the proper system impedance that is a quarter-wave length away, equation 3.1 must be solved. Using Z_0 and Z_{state1} from table 3.1, Z_{state2} is found to be 31.67 - j48.79.

$$Z_{state2} = \frac{Z_0^2}{Z_{state1}} \tag{3.1}$$

It can be seen that 3.1 is a derivative of equation 3.2 when a $l = \frac{\lambda}{4}$.

$$Z_L = Z_0 \frac{Z_{in} - jZ_0 tan\beta l}{Z_0 - jZ_{in} tan\beta l} \tag{3.2}$$

Through using equation 3.3 the desired load impedance can be found. By rearranging the equation and solving for the load impedance, Z_{load} = 1.8559 - j85.4566.

$$\frac{1}{Z_{system}} = \frac{1}{Z_{env}} + \frac{1}{Z_{switch/load}} \tag{3.3}$$

By simulating the system from figure 3.11 in AWR, the Smith chart in figure 3.12 shows the results for the system in both states. The red hourglass shows the impedance of the system with Z_{load}, while the blue triangle shows the impedance of the system for the switch closed, reflective mode.

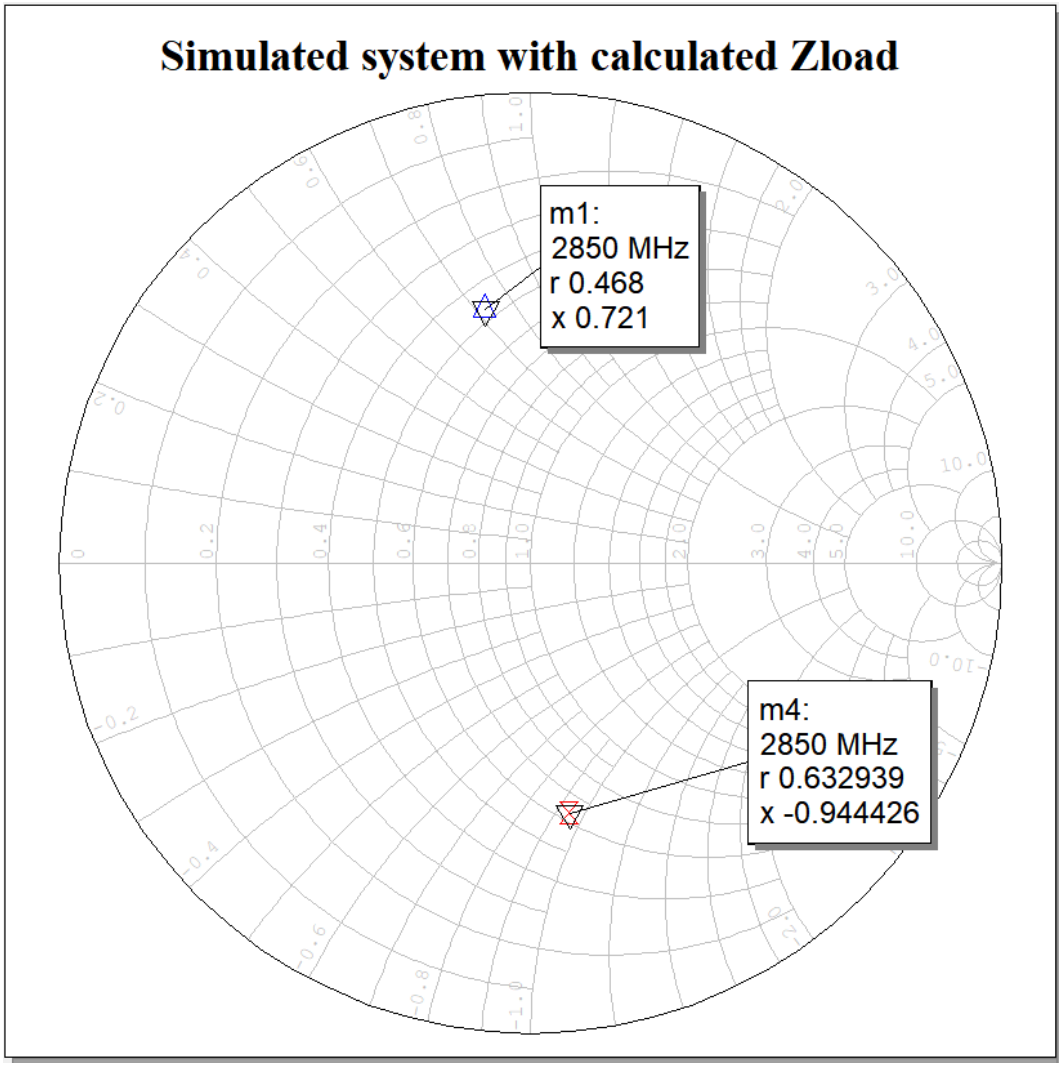

Figure 3.12: Simulated results of AWR transmission line system with calculated load impedance

3.8 Power Budget and Form Factor

To calculate a lifespan of the proposed tag, a power budget table must be made consisting of each component. In table 3.2, each component has its required operation current, as well as, their associated weight. The expected total current required is .7552 mA. The chosen battery for the system is an ECR2450 watch battery, the compromise between size and capacity makes it a good choice. This battery has a typical capacity of 620 mAh, which would give the system a lifespan of 34.2 days without a charging circuit. The final weight of the proposed board was taken by adding the total weight of the components and the weight of a 30 mil 1"x1.5" FR4 board. The size of the board was chosen to accommodate the battery holder which is the largest component. The total weight of the design is 10.988 g. In order to check the viablity of using a tag of this weight a comparison with commercially available RFID tracking tags, such as the Nano backpacks by Telemetry solutions was done. Their nano products range from 5 to 20 g in weight, with their other tracking devices reaching a maximum of 250 g [24].

Table 3.2: Table of components and power requirements

Part Number	Current Used (@3.0 V)	Weight (g)
HMC550ae	200 nA	.016
LTC5505-2	.5 mA	.012
SN74HC393NSR	.08 mA	.2
LMC324AN	.175 mA	.260
ECR2450	N/A	6.8
BU2450SM-JJ-GTR	N/A	2.37

3.9 Conclusion

The parts selected for this study are highly efficient, temperature resistant, and have low power requirements. However, due to the nature of being off the shelf products and readily available they may not be the most ideal selections for a final product. The inability to produce small ceramic antennas and other components requires these parts be used to achieve a reasonable form factor for an RFID tag that could feasibly be attached to a bird. Future considerations for a maximum performance version of this RFID design would benefit from commissioning a 2.85 GHz antenna and potentially other parts used. Nevertheless, The tag still achieves reasonable performance levels to illustrate the concept and to present a working prototype.

Chapter 4

Pulse detection

4.1 Introduction

It is important when considering maximum operation range of the tag to take the incoming WSR-88d pulse's signal strength and subtract system losses. Once the losses have been determined, the strength of the signal going into the envelope detector to be rectified can be calculated. The LTC5055-2 was chosen for this project due to its high sensitivity and low power requirements. From testing done with the entire system put together, it was determined that at 2.85 GHz the RF envelope detector is capable of rectifying signals as low as -10 dBm. From knowing this value, the calculations in chapter 2 were done to determine the maximum range the RFID tag could be from the transmitter. This chapter focuses on what happens to the pulses after they enter the RFID tag.

4.2 Processed WSR-88d pulses and digital logic

Once the RF signal has been rectified to a square wave, the signal is then amplified by a simple op-amp circuit with a gain of 6.8. The newly amplified signal is now

a high enough voltage to trigger the digital counter's clock trigger. Each new pulse follows the same pathway and the counter triggers on the falling edge. The gain can be set to work for the lowest possible voltage the rectifier produces to maximize the range of the system. The voltage can also be set higher to ignore false positives and noise. While setting the gain lower inversely affect the total range, it provides a more stable system that is noise resistant and more reliable. In order to obtain maximum possible range for this study's application, the gain has been set high enough see the calculated -20 dBm pulses that the tag would be receiving around 83 km.

The system operates off standard digital logic. Even though the WSR-88d operates at 2.85 GHz, that is not the frequency the proposed tag modulates at. The 400 Hz - 1.3 KHz separated carrier pulses are what triggers the digital logic. Since standard digital logic chips work into the MHz range, commercially available parts can be use and no special equipment is required. Being able to operate in the KHz range allows for these commercially parts to be used with no error. Additionally, when fabricating the design, it is easier due to the amount of tolerance associated with such low frequencies. In future work, other digital logic parts can be used interchangeably to create different modulation schemes and to create more intricate pulse detection to determine if the incoming pulse is from the WSR-88d. By working with logical ones and zeroes there is a large range of digital logic parts that can be used. Logic gates, counters, flip-flops, and more can all be used new logic designs. This study focused on determining the validity of long range RFID and focused on modulating every other pulse. A standard op-amp circuit and digital counter was used as a simple solution for demonstrating basic capabilities. As

stated in chapter 2, this counter could be extended to allow for more switches and modulation patterns, or could be changed out for a different part to do something more unique with the pulses.

4.3 Specifics of the Envelope Detector

The LTC5505-2 works by holding a base voltage of 0.275V, once a pulse is detected this voltage will temporary spike as the pulse is rectified. This feature is useful for creating digital logic capable of modulating every other pulse and in future work, creating a noise resistant pulse detector. There are a few options when building a trigger schematic and it should be noted that the baseline voltage can be set according to whatever bias is desired. With the temporary increase voltage needed to be used as a trigger there are many options. In the final proposed design, each pulse is amplified by the op-amp circuit and the resulting wave is used to trigger the digital counter. In future work, a comparator could be used to hold one voltage constant with the noise floor detected by the pulse detector to create a more noise resistant form, then pulses would trigger the comparator. This could be done with a higher degree of certainty by using optimized logic parts for this range.

Figure 4.1 shows that the pulse detector holds a constant voltage. From the data sheet, this voltage is based on the input voltage. In this figure it can be seen that the envelope detector holds a constant 273 mV level while it waits to receive a pulse. As pulses are received this voltage temporarily spikes as seen in figure 4.2. For an incoming signal of -10 dBm, the peak voltage is 477 mV, but the oscilloscope shows the average value of the square wave of pulses being received in yellow. In blue the rectified and amplified waves show an average of 2.56 V and a peak of around 3.67

V. As mentioned before, this voltage is high enough to trigger the digital counter.

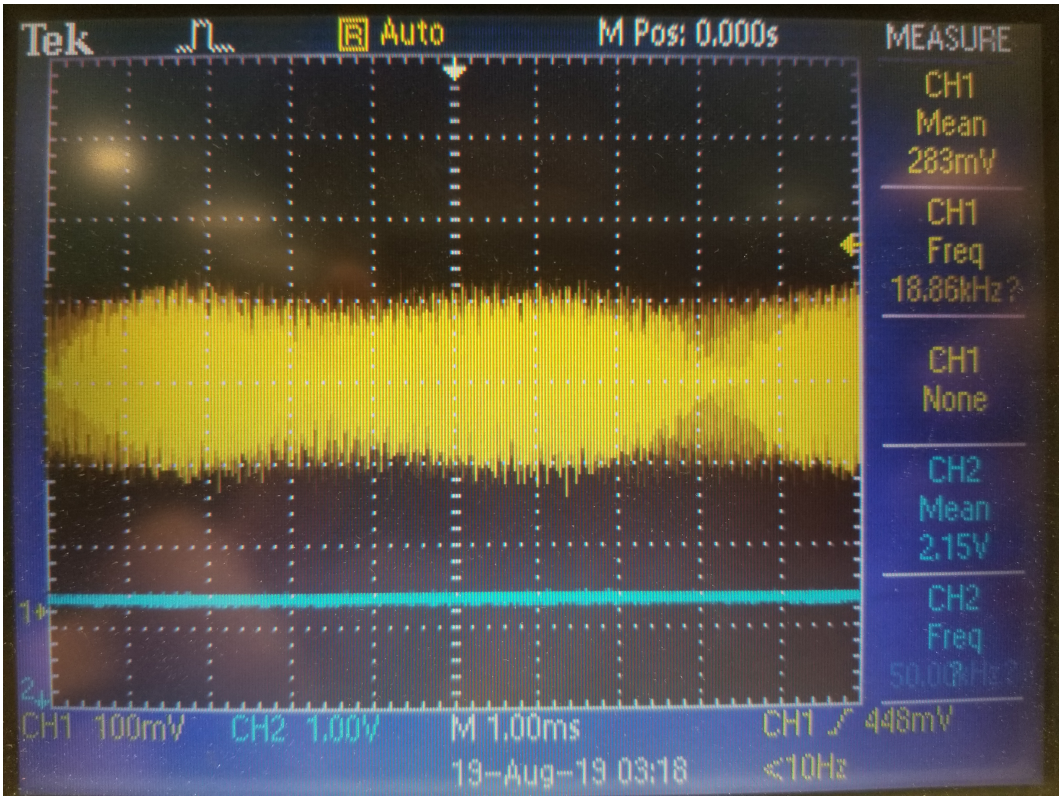

Figure 4.1: Oscilloscope measurements of the envelope detectors output with no incoming pulse.

In figure 4.3 there is a constant -10 dBm wave being generated with no pulse modulation. The envelope detector recognizes that an incoming RF wave is present in yellow, but only triggers once as can be seen by the constant 3.67 V in blue. Without pulse modulation on the incoming signal, the tag does not modulate as expected.

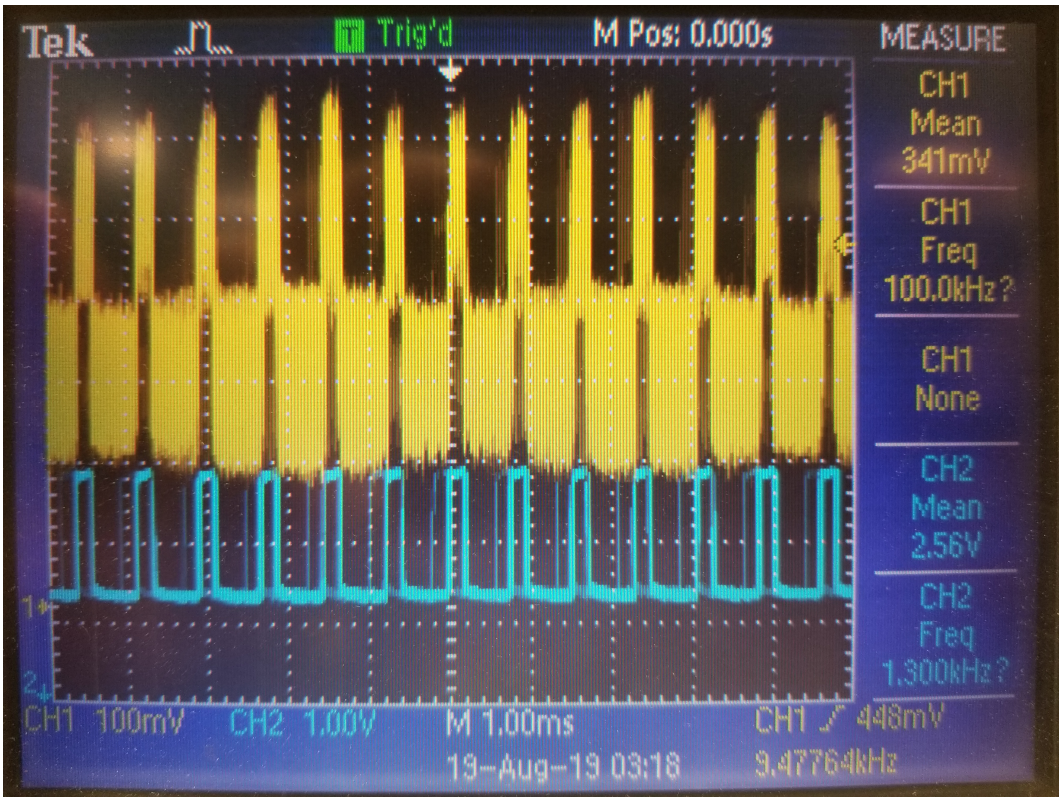

Figure 4.2: Oscilloscope measurements of the envelope detectors output with an incoming pulse train.

In future work, it has been planned to develop a digital logic system that intentionally operates only off of the WSR-88d pulses. By knowing that all WSR-88d pulses are between 500 ns and 1 μs, it is possible to determine if the incoming pulse fits within this time period. Assuming all pulses not falling within this criteria are ignored, the error rate of false positives would go down and the system would be more reliable.

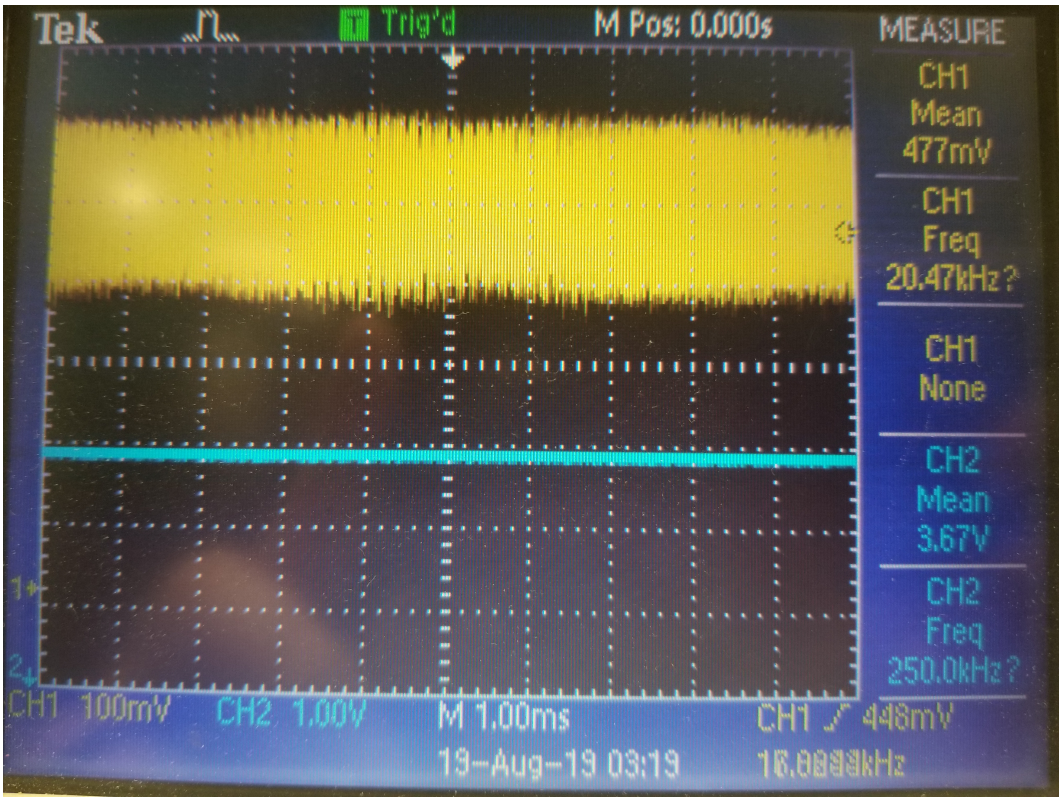

Figure 4.3: Oscilloscope measurements of the envelope detectors output with an incoming continuous signal with no pulse modulation

4.4 Conclusion

The envelope detector chosen for this study works so well that it is not the limiting factor in the design. With the WSR-88d being the limitation on total range due to power received after impinging off the RFID tag. The -20 dBm sensing capabilities of the LTC5055-2 are not necessary and actually out range what the radar is capable of seeing. Due to this factor, in the final design a well tuned amplifier stage could be designed to allow just for the maximum range possible by the system. By matching the distance the RFID tag can detect pulses to the WSR-88d maximum monostatic range and not over amplifying, several benefits can be achieved. An

exact matching of range would also allow for greater filtering of lower level noise and would not require the amplifying stage to be maximized. This would create a more reliable system as false positives from amplifying errant RF noise could be minimized. Combining this tuned amplifying stage with proper WSR-88d pulse detection logic could create an extremely reliable system.

Chapter 5

Proposed tag results

5.1 Introduction

The purpose of this study was to illustrate that the principle techniques of RFID could be implemented in a long range scenario. Since the proposed tag performed as expected from initial designs, long range RFID appears to be viable in a real full scale application. The unique properties of the NEXRAD radar network provide an opportunity to extend this well-documented technology for long range tracking. The results of this study demonstrate the ability to interface RFID technology and the WSR-88d. Such that, the proposed tag is capable of modulating across the entire range of pulses the WSR-88d can produce with a variety of different modulation schemes. The figures detailing modulation across the different PRFs showed that the proposed RFID tag is capable of operating on the NEXRAD's network and is a good starting point for future work. The theoretical range achieved is around 100km in reasonable conditions and provides good tracking coverage on the NEXRAD network.

To illustrate additional future features and their potential implementation with

the network, work was done to detail these multiple standard RFID features that could also be viable at 2.85 GHz. For the purpose of this study, only ASK modulation has been illustrated in this section and detailed. In the future works section there are plans to build and test QAM and other common forms of modulation. The ASK pattern displayed in this section is generated by the digital logic counter and schematic described in section two. The system operates in a fully stand alone form with no additional input other than the signal generator creating the interrogating pulses.

5.2 Results

Overall, the system shows complete functionality at 2.85 GHz with an incoming power level as low as -20 dBm being supplied from the signal generator. This power level should be achievable via transmission according to the Friis equation calculations at 83 km under moderate conditions from section 2. Additionally, the selected hardware is shown to be operable at modulating across the 300 Hz - 1.3 kHz packets with no changes in design. This result is sufficient to show that the tag can operate freely across the entire PRF range the WSR-88d radars output. This study has also shown that all the hardware behind the antenna can be comprised of commercially available components and operate at a highly efficient level. As has been detailed, for this tag to properly reach high ranges, a better antenna with specifications for this project should be design and fabricated.

5.2.1 PRF range and capabilities demonstrations

To fully illustrate the capabilities of the proposed design. The system was tested at a variety of frequencies and two different amplitudes. Figures 5.1, 5.2, and 5.3 show the tag performing with the same modulation scheme at 300 Hz, 1 kHz, and 1.3 kHz. Using figure 5.1 as an example, it can be clearly seen that there is a 5 dB difference in the modulated and non modulated -10 dBm pulses when the switch is terminated into a 50 Ohm load. The figures show that modulation works with an every other pulse (EOP) scheme and the scheme functions with minor variation from pulse to pulse.

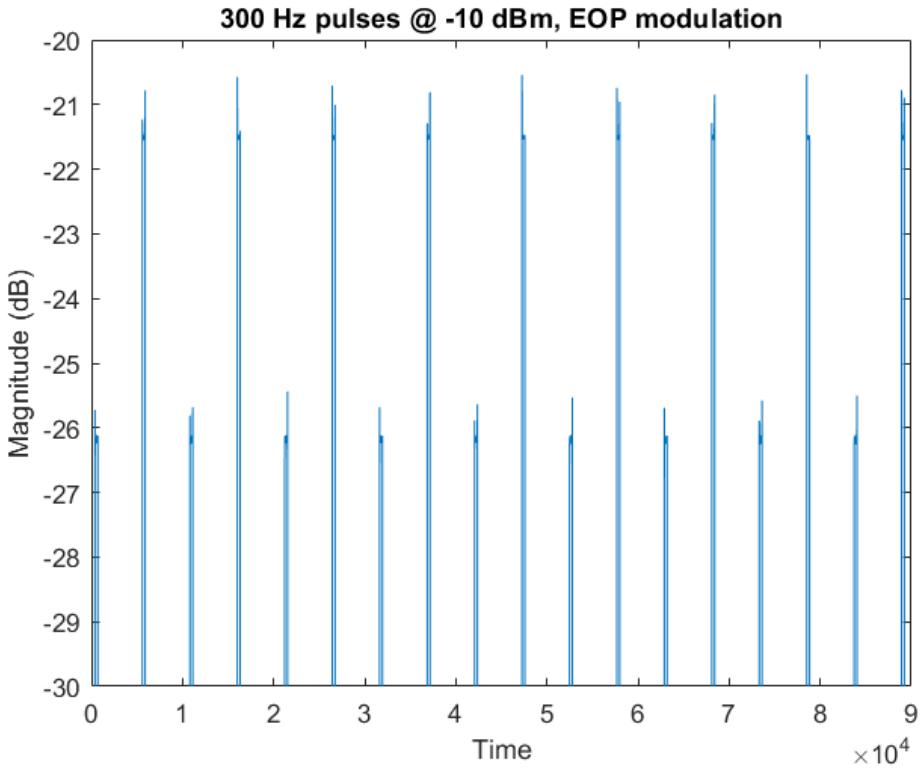

Figure 5.1: 300 Hz pulses 50Ω termination, EOP modulation.

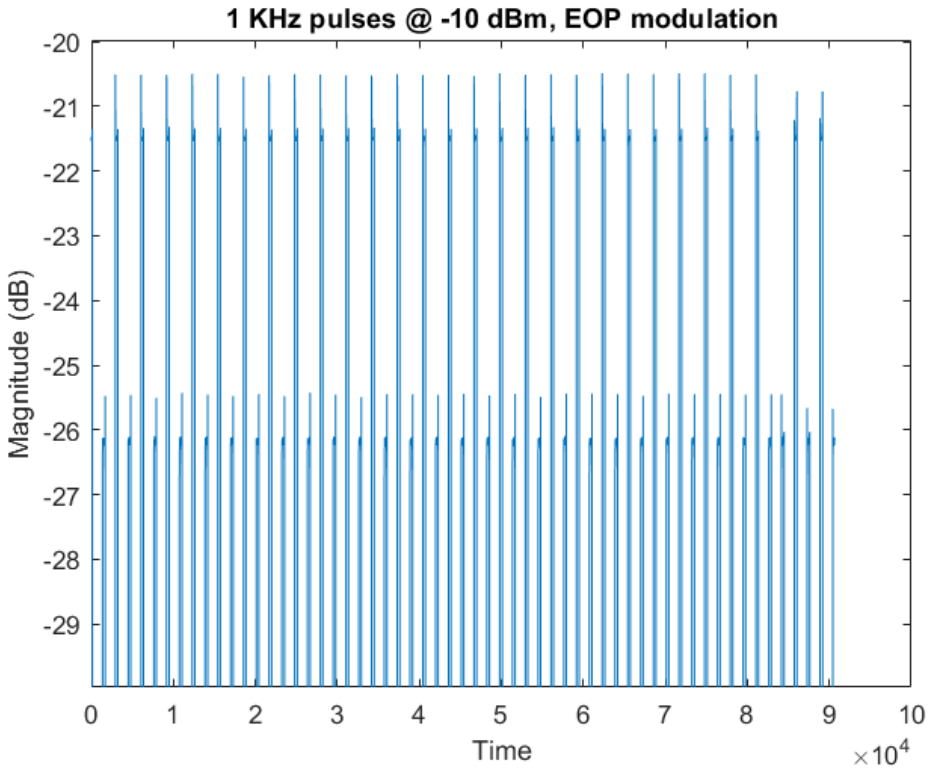

Figure 5.2: 1 KHz pulses 50Ω termination, EOP modulation.

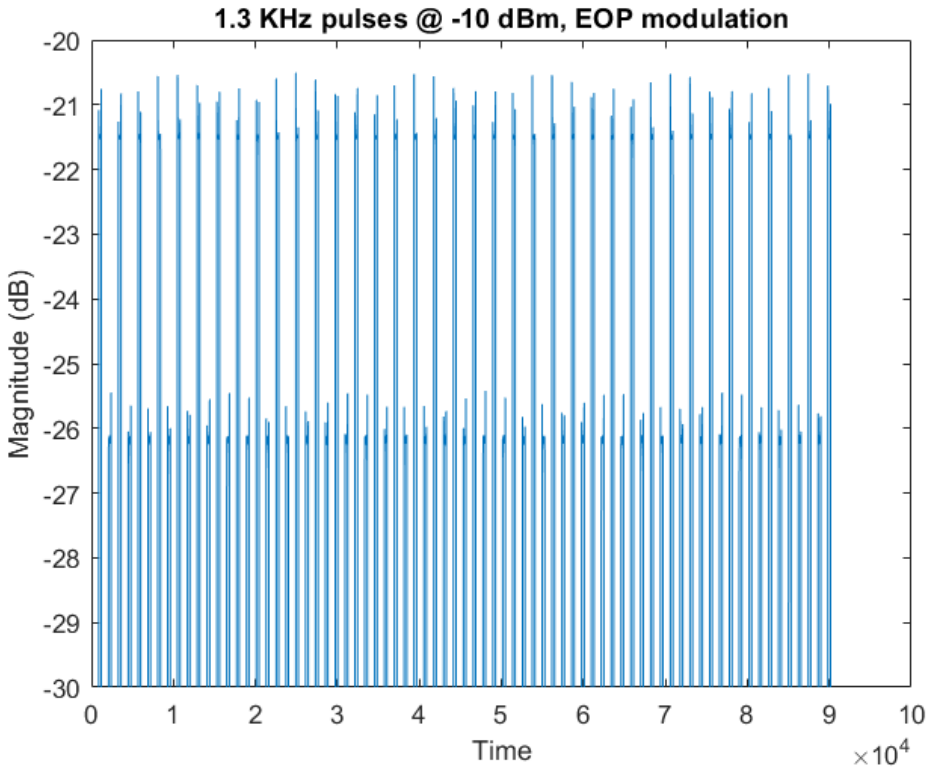

Figure 5.3: 1.3 KHz pulses 50Ω termination, EOP modulation.

5.2.2 Sensitivity examples

Figure 5.4 shows that the modulation works across a variety of incoming pulse power levels with full functionality. It is important to check that the modulation scheme can function properly as the bird flies towards or away from the WSR-88d. Additionally, power sensitivity checks were done with different impedances to check that proper power could be modulated and recognized, even at the lowest end of the detected power spectrum. As seen in figure 5.5 and figure 5.6, the expected amount of modulation can be detected.

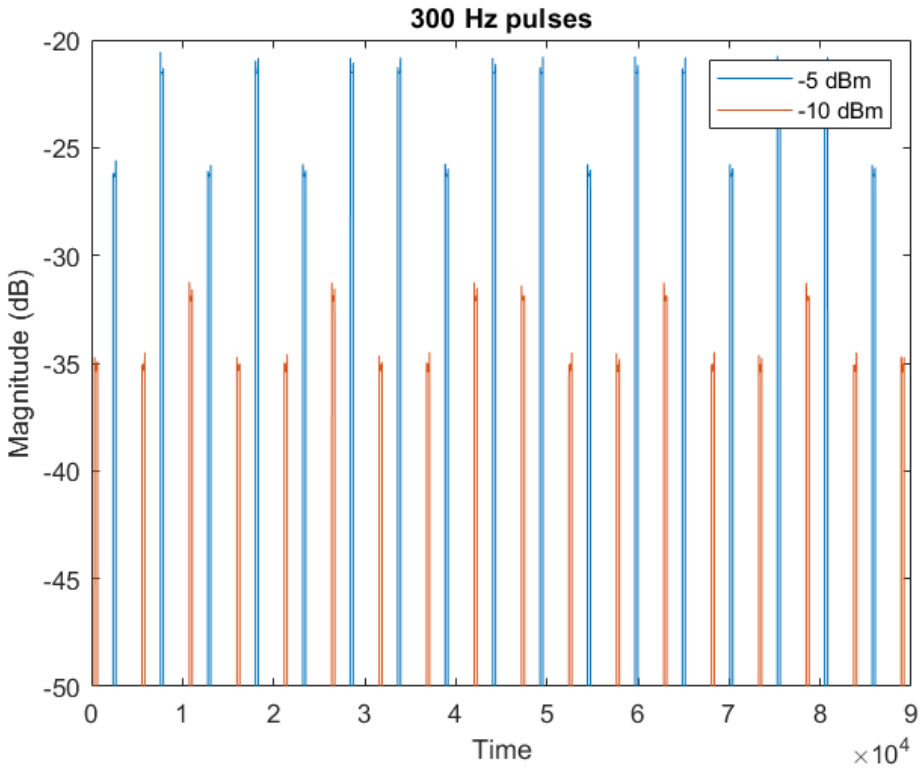

Figure 5.4: 300 Hz pulses through the RFID system at two different power levels.

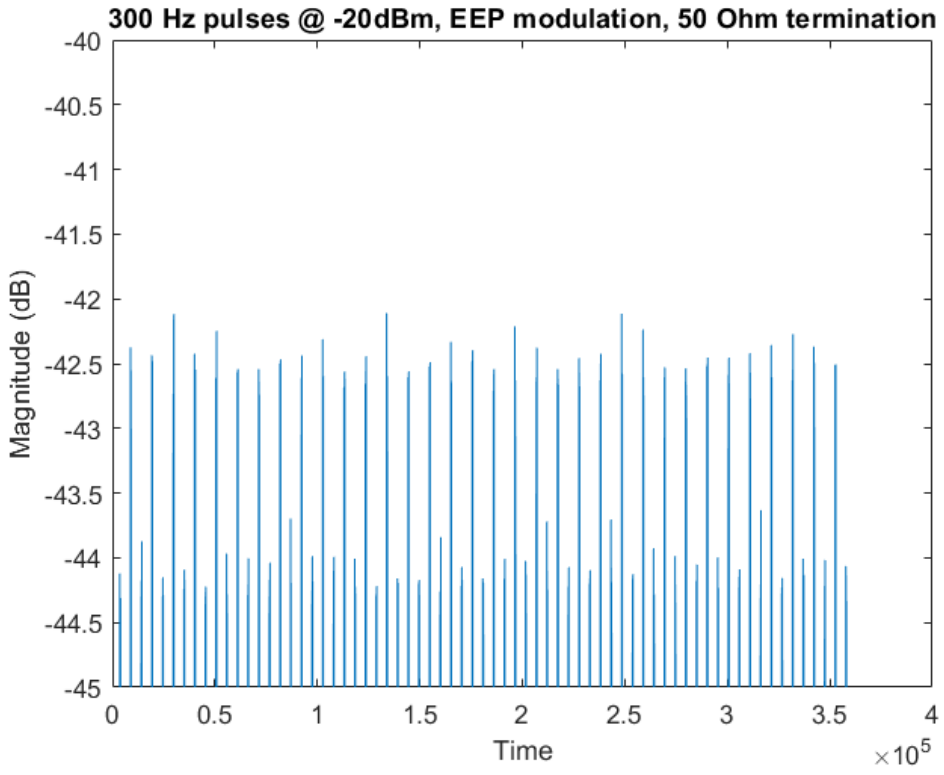

Figure 5.5: 300 Hz pulses through the RFID system with 50Ω termination at -20 dBm

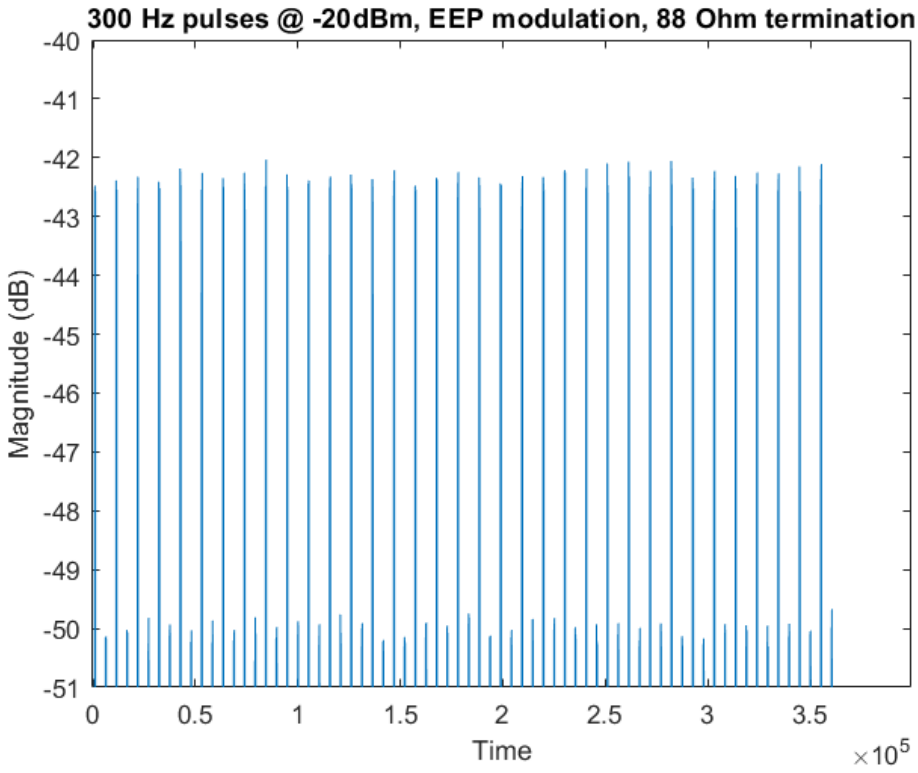

Figure 5.6: 300 Hz pulses through the RFID system with 88Ω termination at -20 dBm

Figure 5.7 shows that when the terminated impedance for the switch is changed, the amount of power backscattered drastically changes as well. There is a 5 dB difference with the 50Ω terminated load, but a 12 dB difference with the 88Ω terminated load. From the calculations done in chapter 2, we see these results follow. These tests were done at -10 dBm to verify their validity among the power spectrum as well.

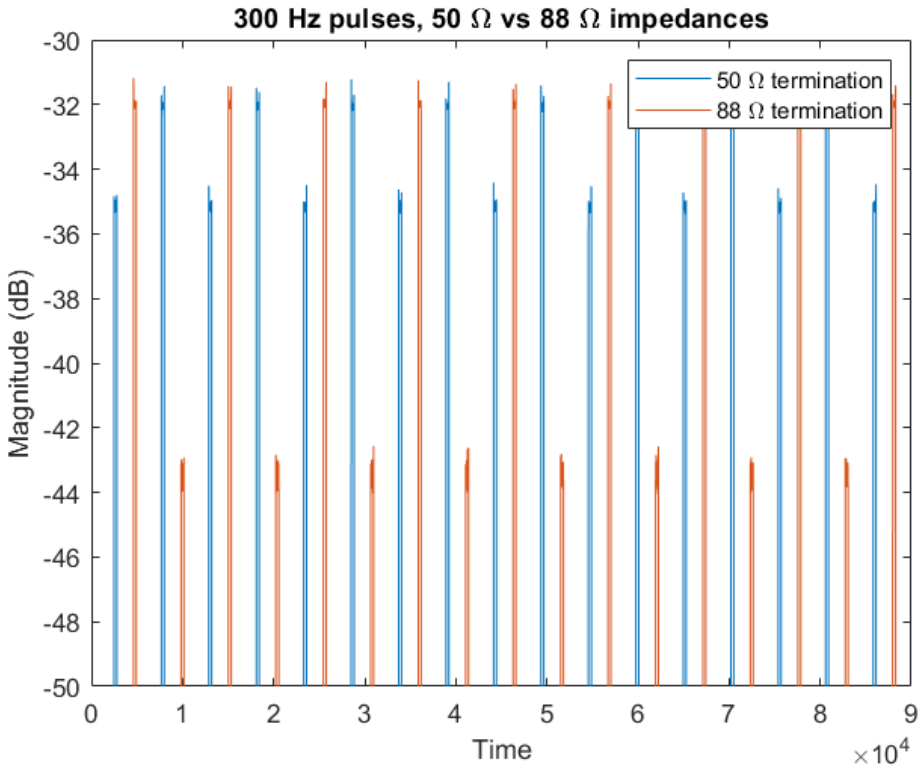

Figure 5.7: 300 Hz pulses through the RFID system with two different impedances.

5.2.3 Modulation Schemes

As discussed in previous chapters, the ability to provide multiple modulation schemes is required for fully operational RFID tags. Figure 5.8 shows the desired every other pulse modulation can be done even at the lowest power level. In figure 5.9 it can be seen that other modulation patterns can also be demonstrated across the same PRF.

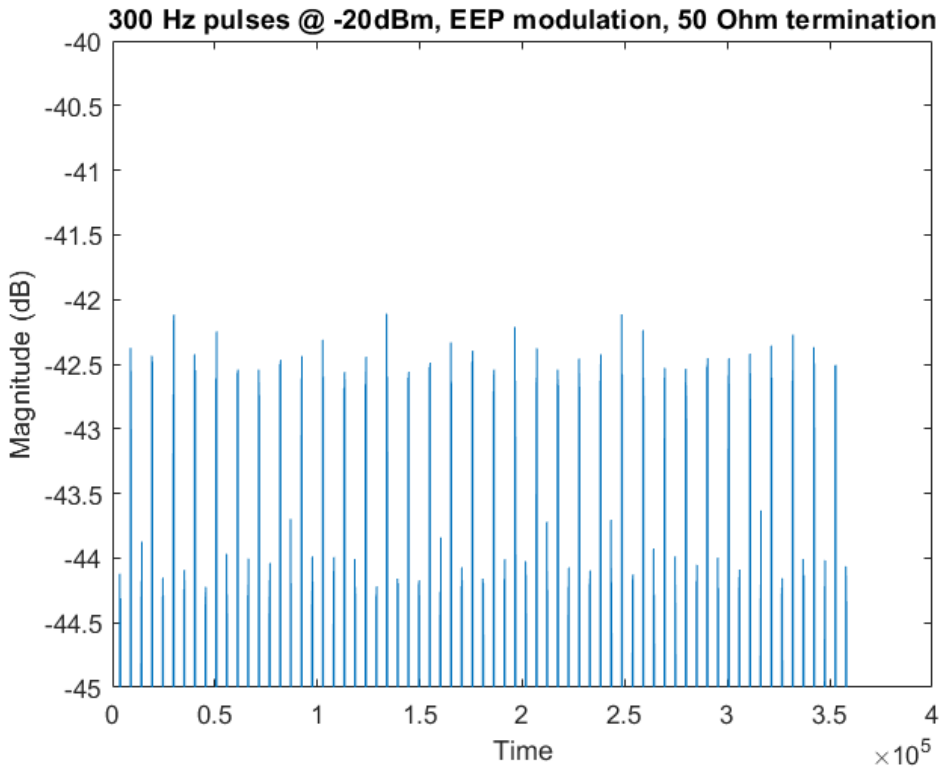

Figure 5.8: 300 Hz pulses with 50Ω termination, EoP modulation.

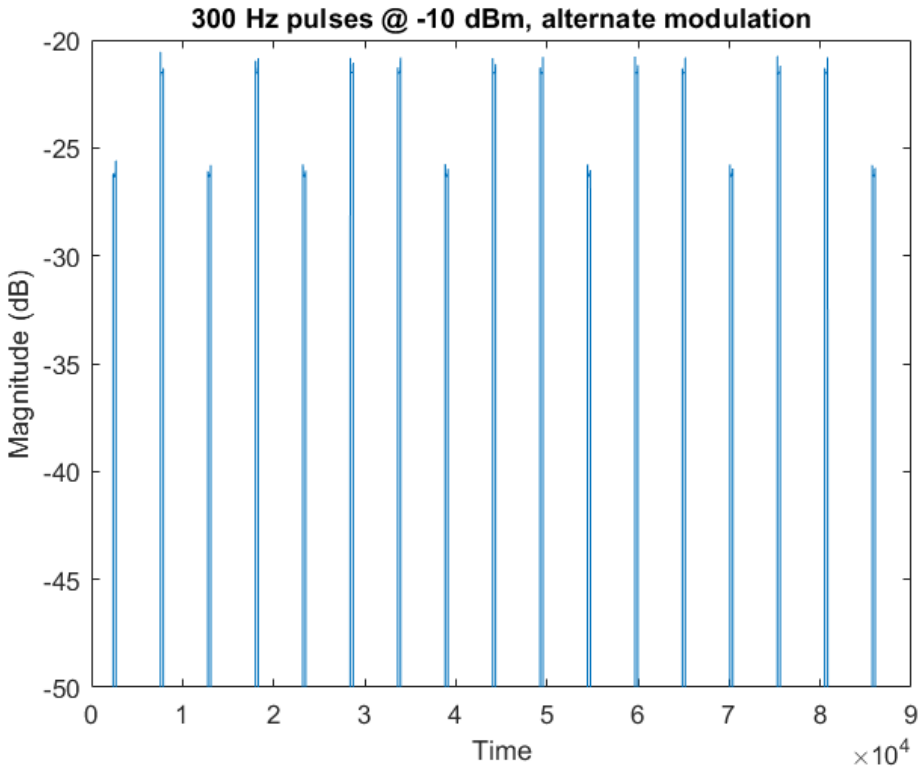

Figure 5.9: 300 Hz pulses 50Ω termination, Alt modulation.

Chapter 6

Conclusions and Future work

6.1 Study Conclusions

Through the results of this study it can be concluded that RFID technology is capable of being utilized at higher frequencies and over large distances. Current RFID technology relies on highly efficient, but low power transmitters that are short range due to federal regulations. The unique characteristics of the NEXRAD network allow for previously unseen distances to be reached due to the enormous amount of power radiated and the high gain of the WSR-88d's aperture. Through the utilization of highly efficient parts and their ability to interface with the WSR-88d it is possible to create a long range RFID network with no infrastructure changes to the NEXRAD network. This study's results thoroughly show that common RFID principles can be applied at higher frequencies given the proper equipment and design. Specifically, ASK backscatter modulation was demonstrated at 2.85 GHz at 300 Hz, 1000 Hz, and 1300 Hz. Additionally, ASK modulation was demonstrated at multiple power levels from 0 dBm to -20 dBm. In order to demonstrate flexibility in digital logic design, multiple ASK schemes were modulated to show the counter's

output could be easily changed to create different patterns to insure unique id's across each tag could be attained.

6.2 Future work

Future considerations for expanding the capabilities of the proposed RFID tag have been made. Due to the results of this study, RFID theory will be applied in future work to test the validity of X-band RFID and to test thoroughly for performance measurements. With the proposed tag utilizing a battery, it follows that the tag would have a finite battery life. The simple solution would be to add a larger battery, but this is not a viable option knowing there is a max capacity the birds being tracked can carry. A viable option has been considered and could be explored in future research, research has been presented and tested to show RF power harvesting on a similar RFID application in the UHF band. RF power harvesting as a way to charge the batteries throughout their life span could greatly increase the life span of the tag at a minimal price and weight cost. A Dickson Rectifier has been specifically used for charging RFID tags in the UHF band[25]. The harvesting system in this capacity was s efficient, there was considerations to remove all batteries from their design. Removing the batteries from this study's proposed design is not viable due to the power being received being a function of range and the random nature of the bird's migration patterns. The difference in range has trade offs, as the birds travel farther from the WSR-88d stations there will less power received and the tags will operate almost entirely off of batteries. As the birds fly closer to the WSR-88d stations we can see through the Friis equation that the power received will be exponentially more, potentially allowing for the tags to charge their batteries quickly.

As mentioned before, due to the random nature of the bird's flight path it is difficult to express the charging efficiency and full charge time explicitly[25].

As mentioned in the conclusion of section 2, fabrication considerations could be made to enhance the capabilities of the system and to fine tune it for 2.85 GHz. By only using COTS, there are some limitations in the parts that can be directly applied. In most cases, there were readily available parts that entirely filled the needed function. However, the antenna was not a perfect match and provides one of the largest sources of inefficiency in the system. An antenna specifically designed to function at 2.85 GHz would be an immediate upgrade to the total system.

Future work also involves an X-band version of the tag. While the range would decrease exponentially, as frequency squared is in the denominator of the fraction, there are a variety of benefits that can potentially be obtained. Less electronic interference is one of the most important benefits. The ability to provide a lower error rate could be very important depending on the application of the X-band RFID tag. Something to consider is that the system does not actually use the higher frequency waveform to communicate. The tag modulates on a pulse to pulse basis, the entire packet of information is modulated across. The 1 KHz carrier packets of 2.85 GHz signal is what are actually being modulated. This could potentially dampen or negate some of the benefits of higher frequency wave forms.

References

[1] E. A. McKinnon and O. P. Love, "Ten years tracking the migrations of small landbirds: Lessons learned in the golden age of bio-logging", *The Auk*, vol. 135, no. 4, pp. 834–856, Jul. 2018, ISSN: 0004-8038. DOI: 10.1642/AUK-17-202.1. eprint: http://oup.prod.sis.lan/auk/article-pdf/135/4/834/28214762/auk0834.pdf. [Online]. Available: https://doi.org/10.1642/AUK-17-202.1.

[2] *NEXRAD description*, 2019. [Online]. Available: https://www.ncdc.noaa.gov/data-access/radar-data/nexrad.

[3] *NEXRAD radar data inventory*, 2019. [Online]. Available: https://www.ncdc.noaa.gov/nexradinv/.

[4] *Maximum RFID power transmitted in the USA*, 2015. [Online]. Available: https://www.law.cornell.edu/cfr/text/47/15.247.

[5] J.-P. Curty, N. Joehl, C. Dehollain, and M. J. Declercq, "Remotely powered addressable UHF RFID integrated system", *IEEE Journal of Solid-State Circuits*, vol. 40, no. 11, pp. 2193–2202, Nov. 2005, ISSN: 0018-9200. DOI: 10.1109/JSSC.2005.857352.

[6] *NEXRAD radar locations*, 2017. [Online]. Available: https://www.roc.noaa.gov/wsr88d/Maps.aspx.

[7] H. Stockman, "Communication by means of reflected power", *Proceedings of the IRE*, vol. 36, no. 10, pp. 1196–1204, Oct. 1948, ISSN: 0096-8390. DOI: 10.1109/JRPROC.1948.226245.

[8] R. F. Harrington, "Theory of loaded scatterers", *Proceedings of the Institution of Electrical Engineers*, vol. 111, no. 4, pp. 617–623, Apr. 1964, ISSN: 0020-3270. DOI: 10.1049/piee.1964.0111.

[9] J. Landt, "The history of rfid", *IEEE Potentials*, vol. 24, no. 4, pp. 8–11, Oct. 2005, ISSN: 0278-6648. DOI: 10.1109/MP.2005.1549751.

[10] A. R. Koelle, S. W. Depp, and R. W. Freyman, "Short-range radio-telemetry for electronic identification, using modulated rf backscatter", *Proceedings of the IEEE*, vol. 63, no. 8, pp. 1260–1261, Aug. 1975, ISSN: 0018-9219. DOI: 10.1109/PROC.1975.9928.

[11] J. D. Griffin and G. D. Durgin, "Complete link budgets for backscatter-radio and RFID systems", *IEEE Antennas and Propagation Magazine*, vol. 51, no. 2, pp. 11–25, Apr. 2009, ISSN: 1045-9243. DOI: 10.1109/MAP.2009.5162013.

[12] K. Finkenzeller, *RFID Handbook*. John Wiley and Sons, Ltd., 2010.

[13] B. Liu and C. Chu, "Security analysis of EPC-enabled RFID network", in *2010 IEEE International Conference on RFID-Technology and Applications*, Jun. 2010, pp. 239–244. DOI: 10.1109/RFID-TA.2010.5529931.

[14] S. Thomas and M. S. Reynolds, "QAM backscatter for passive UHF RFID tags", in *2010 IEEE International Conference on RFID (IEEE RFID 2010)*, Apr. 2010, pp. 210–214. DOI: 10.1109/RFID.2010.5467238.

[15] G. N. Jadhav and S. Hamedi-Hagh, "UHF class-4 active two-way RFID tag for a hybrid RFID-based system", in *2011 IEEE International RF Microwave Conference*, Dec. 2011, pp. 337–342. DOI: 10.1109/RFM.2011.6168762.

[16] R. Correia, N. B. de Carvalho, G. Fukuday, A. Miyaji, and S. Kawasaki, "Backscatter wireless sensor network with WPT capabilities", in *2015 IEEE MTT-S International Microwave Symposium*, May 2015, pp. 1–4. DOI: 10.1109/MWSYM.2015.7166821.

[17] *Commercial RFID tag*. [Online]. Available: https://https://www.esticastresearch.com/wp-content/uploads/2017/10/RFID-Tags-Market-300x180.jpg.

[18] D. K. Cheng, *Field and Wave Electromagnetics*. Pearson Education Limited, 2013.

[19] *Manual of regulations and procedures for federal radio frequency management*, 2017. [Online]. Available: https://www.ntia.doc.gov/page/2011/manual-regulations-and-procedures-federal-radio-frequency-management-redbook.

[20] D. M. Pozar, *Microwave Engineering*. John Wiley and Sons, Inc., 2012.

[21] C. A. Balanis, *Antenna Theory: Analysis and Design*. John Wiley and Sons, Inc, 2005.

[22] J. T. Prothro, *Improved performance of a radio frequency identification tag antenna on a metal ground plane*, 2007.

[23] *Digital counter*, 2019. [Online]. Available: https://www.ibiblio.org/kuphaldt/electricCircuits/Digital/DIGI_11.html.

[24] *Nano backpacks by telemetry solutions*, 2019. [Online]. Available: https://www.telemetrysolutions.com/wildlife-tracking-devices/gps-backpacks/nano-backpacks/.

[25] M. M. Mnif, H. Mnif, and M. Loulou, "New design of RF-DC rectifier circuit for radio frequency energy harvesting", in *2016 IEEE International Conference on Electronics, Circuits and Systems (ICECS)*, Dec. 2016, pp. 664–667. DOI: 10.1109/ICECS.2016.7841289.

[26] R. J. Doviac and D. S. Zrnic, *Doppler Radar and Weather Observations*. Dover Publications Inc., 2006.

[27] *Isu meteorology*, 2019. [Online]. Available: https://www.meteor.iastate.edu/classes/mt432/lectures/ISURadarTalk_NWS_2013.pdf.